Peter Schneider

Extragalactic Astronomy and Cosmology

An Introduction

With 446 figures, including 266 color figures

Springer

Preface

This book began as a series of lecture notes for an introductory astronomy course I have been teaching at the University of Bonn since 2001. This annual lecture course is aimed at students in the first phase of their studies. Most are enrolled in physics degrees and choose astronomy as one of their subjects. This series of lectures forms the second part of the introductory course, and since the majority of students have previously attended the first part, I therefore assume that they have acquired a basic knowledge of astronomical nomenclature and conventions, as well as of the basic properties of stars. Thus, in this part of the course, I concentrate mainly on extragalactic astronomy and cosmology, beginning with a discussion of our Milky Way as a typical (spiral) galaxy. To extend the potential readership of this book to a larger audience, the basics of astronomy and relevant facts about radiation fields and stars are summarized in the appendix.

The goal of the lecture course, and thus also of this book, is to confront physics students with astronomy early in their studies. Since their knowledge of physics is limited in their first year, many aspects of the material covered here need to be explained with simplified arguments. However, it is surprising to what extent modern extragalactic astronomy can be treated with such arguments. All the material in this book is covered in the lecture course, though not all details are written up here. I believe that only by covering this wide range of topics can the students be guided to the forefront of our present astrophysical knowledge. Hence, they learn a lot about issues which are currently not settled and under intense discussion. It is also this aspect which I consider of great importance for the role of astronomy in the framework of a physics program, since in most other sub-disciplines of physics the limits of our current knowledge are approached only at a later stage in the student's education.

In particular, the topic of cosmology is usually met with interest by students. Despite the large amount of material, most of them are able to digest and understand what they are taught, as evidenced from the oral examinations following this course – and this is not small-number statistics: my colleague Klaas de Boer and I together grade about 100 oral examinations per year, covering both parts of the introductory course. Some critical comments coming from students concern the extent of the material as well as its level. However, I do not see a rational reason why the level of an astronomy lecture should be lower than that of one in physics or mathematics.

Why did I turn this into a book? When preparing the concept for my lecture course, I soon noticed that there is no book which I can (or want to) follow. In particular, there are only a few astronomy textbooks in German, and they do not treat extragalactic astronomy and cosmology nearly to the extent and depth as I wanted for this course. Also, the choice of books on these topics in English is fairly limited – whereas a number of excellent introductory textbooks exist, most shy away from technical treatments of issues. However, many aspects can be explained better if a technical argument is also given. Thus I hope that this text presents a field of modern astrophysics at a level suitable for the aforementioned group of people. A further goal is to cover extragalactic astronomy to a level such that the reader should feel comfortable turning to more professional literature.

When being introduced to astronomy, students face two different problems simultaneously. On the one hand, they should learn to understand astrophysical arguments – such as those leading to the conclusion that the central engine in AGNs is a black hole. On the other hand, they are confronted with a multitude of new terms, concepts, and classifications, many of which can only be considered as historical burdens. Examples here are the classification of supernovae which, although based on observational criteria, do not agree with our current understanding of the supernova phenomenon, and the classification of the various types of AGNs. In the lectures, I have tried to separate these two issues, clearly indicating when facts are presented where the students should "just take note", or when astrophysical connections are uncovered which help to understand the properties of cosmic objects. The lat-

ter aspects are discussed in considerably more detail. I hope this distinction can still be clearly seen in this written version.

The order of the material in the course and in this book accounts for the fact that students in their first year of physics studies have a steeply rising learning curve; hence, I have tried to order the material partly according to its difficulty. For example, homogeneous world models are described first, whereas only later are the processes of structure formation discussed, motivated in the meantime by the treatment of galaxy clusters.

The topic and size of this book imply the necessity of a selection of topics. I want to apologize here to all of those colleagues whose favorite subject is not covered at the depth that they feel it deserves. I also took the freedom to elaborate on my own research topic – gravitational lensing – somewhat disproportionately. If it requires a justification: the basic equations of gravitational lensing are sufficiently simple that they and their consequences can be explained at an early stage in astronomy education.

With a field developing as quickly as the subject of this book, it is unavoidable that parts of the text will become somewhat out-of-date quickly. I have attempted to include some of the most recent results of the respective topics, but there are obvious limits. For example, just three weeks before the first half of the manuscript was sent to the publisher the three-year results from WMAP were published. Since these results are compatible with the earlier one-year data, I decided not to include them in this text.

Many students are not only interested in the physical aspects of astronomy, they are also passionate observational astronomers. Many of them have been active in astronomy for years and are fascinated by phenomena occurring beyond the Earth. I have tried to provide a glimpse of this fascination at some points in the lecture course, for instance through some historical details, by discussing specific observations or instruments, or by highlighting some of the great achievements of modern cosmology. At such points, the text may deviate from the more traditional "scholarly" style.

Producing the lecture notes, and their extension to a textbook, would have been impossible without the active help of several students and colleagues, whom I want to thank here. Jan Hartlap, Elisabeth Krause and Anja von der Linden made numerous suggestions for improving the text, produced graphics or searched for figures, and TEXed tables – deep thanks go to them. Oliver Czoske, Thomas Erben and Patrick Simon read the whole German version of the text in detail and made numerous constructive comments which led to a clear improvement of the text. Klaas de Boer and Thomas Reiprich read and commented on parts of this text. Searching for the sources of the figures, Leonardo Castaneda, Martin Kilbinger, Jasmin Pierloz and Peter Watts provided valuable help. A first version of the English translation of the book was produced by Ole Markgraf, and I thank him for this heroic task. Furthermore, Kathleen Schrüfer, Catherine Vlahakis and Peter Watts read the English version and made zillions of suggestions and corrections – I am very grateful to their invaluable help. Thomas Erben, Mischa Schirmer and Tim Schrabback produced the cover image very quickly after our HST data of the cluster RXJ 1347−1145 were taken. Finally, I thank all my colleagues and students who provided encouragement and support for finishing this book.

The collaboration with Springer-Verlag was very fruitful. Thanks to Wolf Beiglböck and Ramon Khanna for their encouragement and constructive collaboration. Bea Laier offered to contact authors and publishers to get the copyrights for reproducing figures – without her invaluable help, the publication of the book would have been delayed substantially. The interaction with LE-TEX, where the book was produced, and in particular with Uwe Matrisch, was constructive as well.

Furthermore, I thank all those colleagues who granted permission to reproduce their figures here, as well as the public relations departments of astronomical organizations and institutes who, through their excellent work in communicating astronomical knowledge to the general public, play an invaluable role in our profession. In addition, they provide a rich source of pictorial material of which I made ample use for this book. Representative of those, I would like to mention the European Southern Observatory (ESO), the Space Telescope Science Institute (STScI), the NASA/SAO/CXC archive for Chandra data and the Legacy Archive for Microwave Background Data Analysis (LAMBDA).

List of Contents

1. Introduction and Overview

1.1 Introduction

The Milky Way, the galaxy in which we live, is but one of many galaxies. As a matter of fact, the Milky Way, also called the Galaxy, is a fairly average representative of the class of spiral galaxies. Two other examples of spiral galaxies are shown in Fig. 1.1 and Fig. 1.2, one of which we are viewing from above (face-on), the other from the side (edge-on). These are all stellar systems in which the majority of stars are confined to a relatively thin disk. In our own Galaxy, this disk can be seen as the band of stars stretched across the night sky, which led to it being named the Milky Way. Besides such disk galaxies, there is a second major class of luminous stellar systems, the elliptical galaxies. Their properties differ in many respects from those of the spirals.

It was less than a hundred years ago that astronomers first realized that objects exist outside our Milky Way and that our world is significantly larger than the size of the Milky Way. In fact, galaxies are mere islands in the Universe: the diameter of our Galaxy[1] (and other galaxies) is much smaller than the average separation between luminous galaxies. The discovery of the existence of other stellar systems and their variety of morphologies raised the question of the origin and evolution of these galaxies. Is there anything between the galaxies, or is it just empty space? Are there any other cosmic bodies besides galaxies? Questions like these motivated us to explore the Universe as a whole and its evolution. Is our

[1] We shall use the terms "Milky Way" and "Galaxy" synonymously throughout.

Fig. 1.1. The spiral galaxy NGC 1232 may resemble our Milky Way if it were to be observed from "above" (face-on). This image, observed with the VLT, has a size of $6.'8 \times 6.'8$, corresponding to a linear size of 60 kpc at its distance of 30 Mpc. If this was our Galaxy, our Sun would be located at a distance of 8.0 kpc from the center, orbiting around it at a speed of ~ 220 km/s. A full revolution would take us about 230×10^6 years. The bright knots seen along the spiral arms of this galaxy are clusters of newly-formed stars, similar to bright young star clusters in our Milky Way. The different, more reddish, color of the inner part of this galaxy indicates that the average age of the stars there is higher than in the outer parts. The small galaxy at the lower left edge of the image is a companion galaxy that is distorted by the gravitational tidal forces caused by the spiral galaxy

Peter Schneider, Introduction and Overview.
In: Peter Schneider, Extragalactic Astronomy and Cosmology. pp. 1–33 (2006)
DOI: 10.1007/11614371_1

Fig. 1.2. We see the spiral galaxy NGC 4013 from the side (edge-on); an observer looking at the Milky Way from a direction which lies in the plane of the stellar disk ("from the side") may have a view like this. The disk is clearly visible, with its central region obscured by a layer of dust. One also sees the central bulge of the galaxy. As will be discussed at length later on, spiral galaxies like this one are surrounded by a halo of matter which is observed only through its gravitational action, e.g., by affecting the velocity of stars and gas rotating around the center of the galaxy

Universe finite or infinite? Does it change over time? Does it have a beginning and an end? Mankind has long been fascinated by these questions about the origin and the history of our world. But for only a few decades have we been able to approach these questions in an empirical manner. As we shall discuss in this book, many of the questions have now been answered. However, each answer raises yet more questions, as we aim towards an ever increasing understanding of the physics of the Universe.

The stars in our Galaxy have very different ages. The oldest stars are about 12 billion years old, whereas in some regions stars are still being born today: for instance in the well-known Orion nebula. Obviously, the stellar content of our Galaxy has changed over time. To understand the formation and evolution of the Galaxy a view of its (and thus our own) past would be useful. Unfortunately, this is physically impossible. However, due to the finite speed of light, we see objects at large distances in an earlier state, as they were in the past. One can now try to identify and analyze such distant galaxies, which may have been the progenitors of galaxies like our own Galaxy, in this way reconstructing the main aspects of the history of the Milky Way. We will never know the exact initial conditions that led to the evolution of the Milky Way, but we may be able to find some characteristic conditions. Emerging from such initial states, cosmic evolution should produce galaxies similar to our own, which we would then be able to observe from the outside. On the other hand, only within our own Galaxy can we study the physics of galaxy evolution *in situ*.

We are currently witnessing an epoch of tremendous discoveries in astronomy. The technical capabilities in observation and data reduction are currently evolving at an enormous pace. Two examples taken from ground-based optical astronomy should serve to illustrate this.

In 1993 the first 10-m class telescope, the Keck telescope, was commissioned, the first increase in light-collecting power of optical telescopes since the completion of the 5-m mirror on Mt. Palomar in 1948. Now, just a decade later, about ten telescopes of the 10-m class are in use, and even more are soon to come. In recent years, our capabilities to find very distant, and thus very dim, objects and to examine them in detail have improved immensely thanks to the capability of these large optical telescopes.

A second example is the technical evolution and size of optical detectors. Since the introduction of CCDs in astronomical observations at the end of the 1970s, which replaced photographic plates as optical detectors, the sensitivity, accuracy, and data rate of optical observations have increased enormously. At the end of the 1980s, a camera with 1000×1000 pixels (*pic*ture *el*ement*s*) was considered a wide-field instrument. In 2003 a camera called Megacam began operating; it has $(18\,000)^2$ pixels and images a square degree of the sky at a sampling rate of $0\farcs2$ in a single exposure. Such a camera produces roughly 100 GB of data every night, the reduction of which requires fast computers and vast storage capacities. But it is not only optical astronomy that is in a phase of major development; there has also been huge progress in instrumentation in other wavebands. Space-based observing platforms are playing

a crucial role in this. We will consider this topic in Sect. 1.3.

These technical advances have led to a vast increase in knowledge and insight in astronomy, especially in extragalactic astronomy and cosmology. Large telescopes and sensitive instruments have opened up a window to the distant Universe. Since any observation of distant objects is inevitably also a view into the past, due to the finite speed of light, studying objects in the early Universe has become possible. Today, we can study galaxies which emitted the light we observe at a time when the Universe was less than 10% of its current age; these galaxies are therefore in a very early evolutionary stage. We are thus able to observe the evolution of galaxies throughout the past history of the Universe. We have the opportunity to study the history of galaxies and thus that of our own Milky Way. We can examine at which epoch most of the stars that we observe today in the local Universe have formed because the history of star formation can be traced back to early epochs. In fact, it has been found that star formation is largely hidden from our eyes and only observable with space-based telescopes operating in the far-infrared waveband.

One of the most fascinating discoveries of recent years is that most galaxies harbor a black hole in their center, with a characteristic mass of millions or even billions of solar masses – so-called supermassive black holes. Although as soon as the first quasars were found in 1963 it was proposed that only processes around a supermassive black hole would be able to produce the huge amount of energy emitted by these ultra-luminous objects, the idea that such black holes exist in normal galaxies is fairly recent. Even more surprising was the finding that the black hole mass is closely related to the other properties of its parent galaxy, thus providing a clear indication that the evolution of supermassive black holes is closely linked to that of their host galaxies.

Detailed studies of individual galaxies and of associations of galaxies, which are called galaxy groups or clusters of galaxies, led to the surprising result that these objects contain considerably more mass than is visible in the form of stars and gas. Analyses of the dynamics of galaxies and clusters show that only 10–20% of their mass consists of stars, gas and dust that we are able to observe in emission or absorption. The largest fraction of their mass, however, is invisible. Hence, this hidden mass is called *dark matter*. We know of its presence only through its gravitational effects. The dominance of dark matter in galaxies and galaxy clusters was established in recent years from observations with radio, optical and X-ray telescopes, and it was also confirmed and quantified by other methods. However, we do not know what this dark matter consists of; the unambiguous evidence for its existence is called the "dark matter problem".

The nature of dark matter is one of the central questions not only in astrophysics but also poses a challenge to fundamental physics, unless the "dark matter problem" has an astronomical solution. Does dark matter consist of non-luminous celestial bodies, for instance burned-out stars? Or is it a new kind of matter? Have astronomers indirectly proven the existence of a new elementary particle which has thus far escaped detection in terrestrial laboratories? If dark matter indeed consists of a new kind of elementary particle, which is the common presumption today, it should exist in the Milky Way as well, in our immediate vicinity. Therefore, experiments which try to directly detect the constituents of dark matter with highly sensitive and sophisticated detectors have been set up in underground laboratories. Physicists and astronomers are eagerly awaiting the commissioning of the Large Hadron Collider (LHC), a particle accelerator at the European CERN research center which, from 2007 on, will produce particles at significantly higher energies than accessible today. The hope is to find an elementary particle that could serve as a candidate constituent of dark matter.

Without doubt, the most important development in recent years is the establishment of a standard model of cosmology, i.e., the science of the Universe as a whole. The Universe is known to expand and it has a finite age; we now believe that we know its age with a precision of as little as a few percent – it is $t_0 = 13.7$ Gyr. The Universe has evolved from a very dense and very hot state, the Big Bang, expanding and cooling over time. Even today, echoes of the Big Bang can be observed, for example in the form of the cosmic microwave background radiation. Accurate observations of this background radiation, emitted some 380 000 years after the Big Bang, have made an important contribution to what we know today about the composition of the Universe. However, these results raise more questions than they answer: only $\sim 4\%$ of the energy content of the Universe can be accounted for by matter which is well-known from

other fields of physics, the *baryonic matter* that consists mainly of atomic nuclei and electrons. About 25% of the Universe consists of dark matter, as we already discussed in the context of galaxies and galaxy clusters. Recent observational results have shown that the mean density of dark matter dominates over that of baryonic matter also on cosmic scales.

Even more surprising than the existence of dark matter is the discovery that about 70% of the Universe consists of something that today is called vacuum energy, or dark energy, and that is closely related to the cosmological constant introduced by Albert Einstein. The fact that various names do exist for it by no means implies that we have any idea what this dark energy is. It reveals its existence exclusively in its effect on cosmic expansion, and it even dominates the expansion dynamics at the current epoch. Any efforts to estimate the density of dark energy from fundamental physics have failed hopelessly. An estimate of the vacuum energy density using quantum mechanics results in a value that is roughly *120 orders of magnitude* larger than the value derived from cosmology. For the foreseeable future observational cosmology will be the only empirical probe for dark energy, and an understanding of its physical nature will probably take a substantial amount of time. The existence of dark energy may well pose the greatest challenge to fundamental physics today.

In this book we will present a discussion of the extragalactic objects found in astronomy, starting with the Milky Way which, being a typical spiral galaxy, is considered a prototype of this class of stellar systems. The other central topic in this book is a presentation of modern astrophysical cosmology, which has experienced tremendous advances in recent years. Methods and results will be discussed in parallel. Besides providing an impression of the fascination that arises from astronomical observations and cosmological insights, astronomical methods and physical considerations will be our prime focus. We will start in the next section with a concise overview of the fields of extragalactic astronomy and cosmology. This is, on the one hand, intended to whet the reader's appetite and curiosity, and on the other hand to introduce some facts and technical terms that will be needed in what follows but which are discussed in detail only later in the book. In Sect. 1.3 we will describe some of the most important telescopes used in extragalactic astronomy today.

1.2 Overview

1.2.1 Our Milky Way as a Galaxy

The Milky Way is the only galaxy which we are able to examine in detail. We can resolve individual stars and analyze them spectroscopically. We can perform detailed studies of the interstellar medium (ISM), such as the properties of molecular clouds and star-forming regions. We can quantitatively examine extinction and reddening by dust. Furthermore, we can observe the local dynamics of stars and gas clouds as well as the properties of satellite galaxies (such the Magellanic Clouds). Finally, the Galactic center at a distance of only 8 kpc[2] gives us the unique opportunity to examine the central region of a galaxy at very high resolution. Only through a detailed understanding of our own Galaxy can we hope to understand the properties of other galaxies. Of course, we implicitly assume that the physical processes taking place in other galaxies obey the same laws of physics that apply to us. If this were not the case, we would barely have a chance to understand the physics of other objects in the Universe, let alone the Universe as a whole. We will return to this point shortly.

We will first discuss the properties of our own Galaxy. One of the main problems here, and in astronomy in general, is the determination of the distance to an object. Thus we will start by considering this topic. From the analysis of the distribution of stars and gas in the Milky Way we will then derive its structure. It is found that the Galaxy consists of several distinct components:

- a thin disk of stars and gas with a radius of about 20 kpc and a scale-height of about 300 pc, which also hosts the Sun;
- a $\sim$ 1 kpc thick disk, which contains a different stellar population compared to the thin disk;
- a central bulge, as is also found in other spiral galaxies;
- and a nearly spherical halo which contains most of the globular clusters and some old stars.

Figure 1.3 shows a schematic view of our Milky Way and its various components. For a better visual impression, Figs. 1.1 and 1.2 show two spiral galaxies, the

[2] One parsec (1 pc) is the common unit of distance in astronomy, with 1 pc = 3.086×10^{18} cm. Also used are 1 kpc = 10^3 pc, 1 Mpc = 10^6 pc, 1 Gpc = 10^9 pc. Other commonly used units and constants are listed in Appendix C.

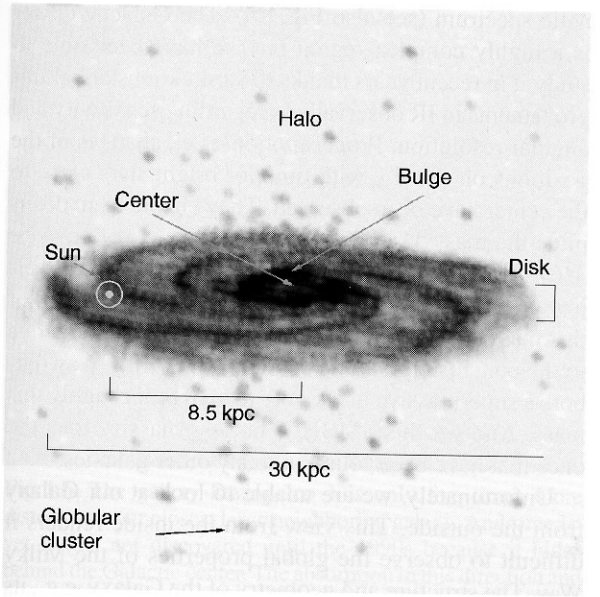

Fig. 1.3. Schematic structure of the Milky Way consisting of the disk, the central bulge with the Galactic center, and the spherical halo in which most of the globular clusters are located. The Sun orbits around the Galactic center at a distance of about 8 kpc

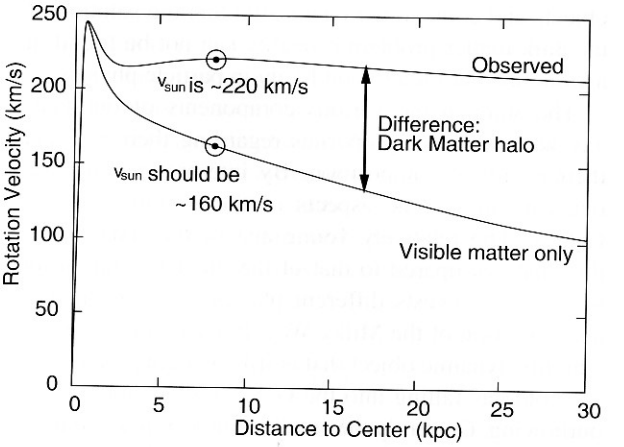

Fig. 1.4. The upper curve is the observed rotation curve $V(R)$ of our Galaxy, i.e., the rotational velocity of stars and gas around the Galactic center as a function of their galacto-centric distance. The lower curve is the rotation curve that we would predict based solely on the observed stellar mass of the Galaxy. The difference between these two curves is ascribed to the presence of dark matter, in which the Milky Way disk is embedded

former viewed from "above" (face-on) and the latter from the "side" (edge-on). In the former case, the spiral structure, from which this kind of galaxy derives its name, is clearly visible. The bright knots in the spiral arms are regions where young, luminous stars have recently formed. The image shows an obvious color gradient: the galaxy is redder in the center and bluest in the spiral arms – while star formation is currently taking place in the spiral arms, we find mainly old stars towards the center, especially in the bulge.

The Galactic disk rotates, with rotational velocity $V(R)$ depending on the distance R from the center. We can estimate the mass of the Galaxy from the distribution of the stellar light and the mean mass-to-light ratio of the stellar population, since gas and dust represent less than $\sim 10\%$ of the mass of the stars. From this mass estimate we can predict the rotational velocity as a function of radius simply from Newtonian mechanics. However, the observed rotational velocity of the Sun around the Galactic center is significantly higher than would be expected from the observed mass distribution. If $M(R_0)$ is the mass inside a sphere around the Galactic center with radius $R_0 \approx 8$ kpc, then the rotational velocity from Newtonian mechanics[3] is

$$V_0 = \sqrt{\frac{G\,M(R_0)}{R_0}}\,. \tag{1.1}$$

From the visible matter in stars we would expect a rotational velocity of ~ 160 km/s, but we observe $V_0 \sim 220$ km/s (see Fig. 1.4). This, and the shape of the rotation curve $V(R)$ for larger distances R from the Galactic center, indicates that our Galaxy contains significantly more mass than is visible in the form of stars.[4] This additional mass is called *dark matter*. Its physical nature is still unknown. The main candidates are weakly interacting elementary particles like those postulated by some elementary particle theories, but they have yet not been detected in the laboratory. Macroscopic objects (i.e., celestial bodies) are also in principle possible candidates if they emit very little light. We will discuss experiments which allow us to identify such macroscopic

[3] We use standard notation: G is the Newtonian gravitational constant, c the speed of light.

[4] Strictly speaking, (1.1) is valid only for a spherically symmetric mass distribution. However, the rotational velocity for an oblate density distribution does not differ much, so we can use this relation as an approximation.

objects and come to the conclusion that the solution of the dark matter problem probably can not be found in astronomy, but rather most likely in particle physics.

The stars in the various components of our Galaxy have different properties regarding their age and their chemical composition. By interpreting this fact one can infer some aspects of the evolution of the Galaxy. The relatively young age of the stars in the thin disk, compared to that of the older population in the bulge, suggests different phases in the formation and evolution of the Milky Way. Indeed, our Galaxy is a highly dynamic object that is still changing today. We see cold gas falling into the Galactic disk and hot gas outflowing. Currently the small neighboring Sagittarius dwarf galaxy is being torn apart in the tidal gravitational field of the Milky Way and will merge with it in the (cosmologically speaking) near future.

One cannot see far through the disk of the Galaxy at optical wavelengths due to extinction by dust. Therefore, the immediate vicinity of the Galactic center can be examined only in other wavebands, especially the infrared (IR) and the radio parts of the electromagnetic spectrum (see also Fig. 1.5). The Galactic center is a highly complex region but we have been able to study it in recent years thanks to various substantial improvements in IR observations regarding sensitivity and angular resolution. Proper motions, i.e., changes of the positions on the sky with time, of bright stars close to the center have been observed. They enable us to determine the mass M in a volume of radius ~ 0.1 pc to be $M(0.1\ \mathrm{pc}) \sim 3 \times 10^6\ M_\odot$. Although the data do not allow us to make a totally unambiguous interpretation of this mass concentration there is no plausible alternative to the conclusion that the center of the Milky Way harbors a supermassive black hole (SMBH) of roughly this mass. And yet this SMBH is far less massive than the ones that have been found in many other galaxies.

Unfortunately, we are unable to look at our Galaxy from the outside. This view from the inside renders it difficult to observe the global properties of the Milky Way. The structure and geometry of the Galaxy, e.g., its spiral arms, are hard to identify from our location. In addition, the extinction by dust hides large parts of the Galaxy from our view (see Fig. 1.6), so that the global

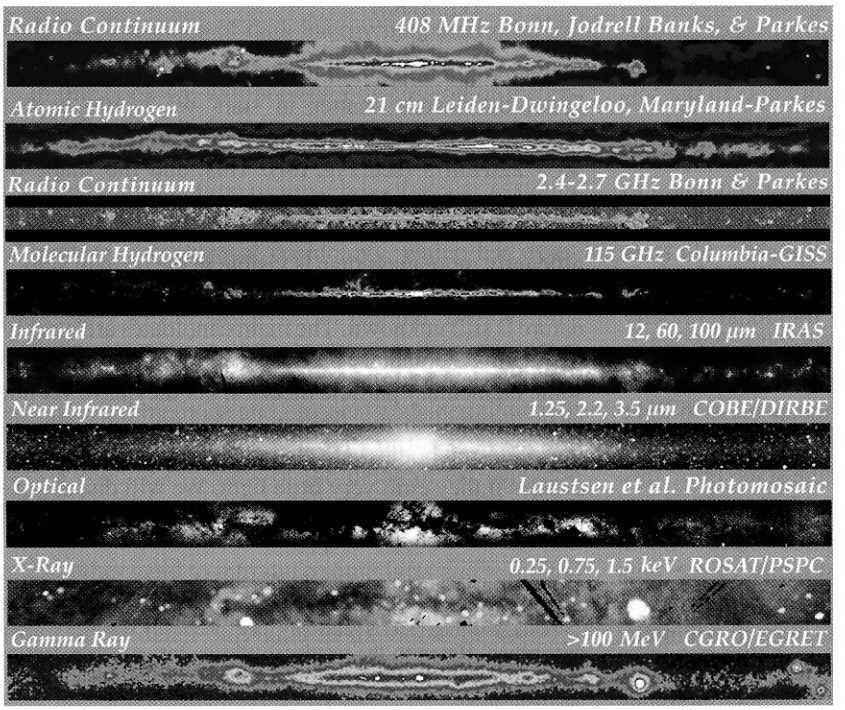

Fig. 1.5. The Galactic disk observed in nine different wavebands. Its appearance differs strongly in the various images; for example, the distribution of atomic hydrogen and of molecular gas is much more concentrated towards the Galactic plane than the distribution of stars observed in the near-infrared, the latter clearly showing the presence of a central bulge. The absorption by dust at optical wavelengths is also clearly visible and can be compared to that in Fig. 1.2

Fig. 1.6. The galaxy Dwingeloo 1 is only five times more distant than our closest large neighboring galaxy, Andromeda, yet it was not discovered until the 1990s because it hides behind the Galactic center. The absorption in this direction and numerous bright stars prevented it being discovered earlier. The figure shows an image observed with the Isaac Newton Telescope in the V-, R-, and I-bands

parameters of the Milky Way (like its total luminosity) are difficult to measure. These parameters are estimated much better from outside, i.e., in other similar spiral galaxies. In order to understand the large-scale properties of our Galaxy, a comparison with similar galaxies which we can examine in their entirety is extremely helpful. Only by combining the study of the Milky Way with that of other galaxies can we hope to fully understand the physical nature of galaxies and their evolution.

1.2.2 The World of Galaxies

Next we will discuss the properties of other galaxies. The two main types of galaxies are spirals (like the Milky Way, see also Fig. 1.7) and elliptical galaxies (Fig. 1.8). Besides these, there are additional classes such as irregular and dwarf galaxies, active galaxies, and starburst galaxies, where the latter have a very high star-formation rate in comparison to normal galaxies. These classes differ not only in their morphology, which forms the basis for their classification, but also in their physical properties such as color (indicating a different stellar content), internal reddening (depending on their dust

Fig. 1.7. NGC 2997 is a typical spiral galaxy, with its disk inclined by about 45° with respect to the line-of-sight. Like most spiral galaxies it has two spiral arms; they are significantly bluer than other parts of the galaxy. This is caused by ongoing star formation in these regions so that young, hot and thus blue stars are present in the arms, whereas the center of the galaxy, especially the bulge, consists mainly of old stars

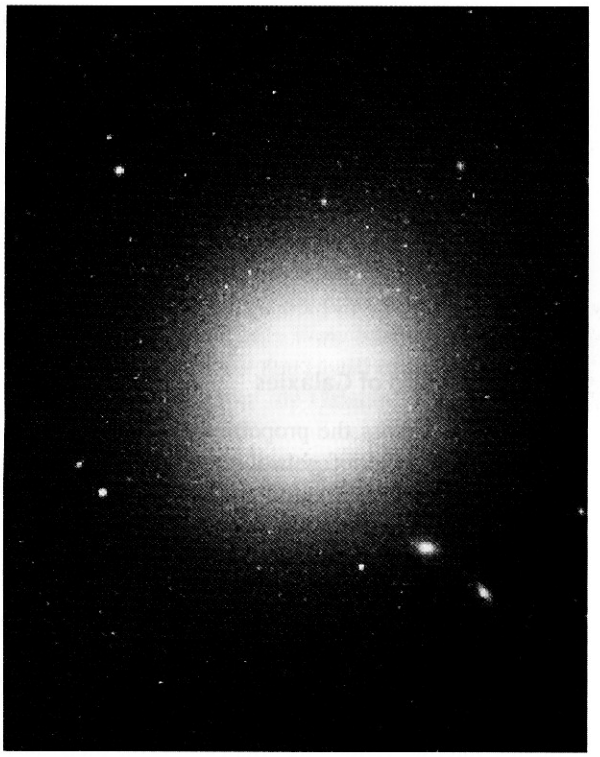

Fig. 1.8. M87 is a very luminous elliptical galaxy in the center of the Virgo Cluster, at a distance of about 18 Mpc. The diameter of the visible part of this galaxy is about 40 kpc; it is significantly more massive than the Milky Way ($M > 3 \times 10^{12} M_{\odot}$). We will frequently refer to this galaxy: it is not only an excellent example of a central cluster galaxy but also a representative of the family of "active galaxies". It is a strong radio emitter (radio astronomers also know it as Virgo A), and it has an optical jet in its center

content), amount of interstellar gas, star-formation rate, etc. Galaxies of different morphologies have evolved in different ways.

Spiral galaxies are stellar systems in which active star formation is still taking place today, whereas elliptical galaxies consist mainly of old stars – their star formation was terminated a long time ago. The S0 galaxies, an intermediate type, show a disk similar to that of spiral galaxies but like ellipticals they consist mainly of old stars, i.e., stars of low mass and low temperature. Ellipticals and S0 galaxies together are often called *early-type galaxies*, whereas spirals are termed *late-type galaxies*. These names do not imply any interpretation but exist only for historical reasons.

The disks of spiral galaxies rotate differentially. As for the Milky Way, one can determine the mass from the rotational velocity using the Kepler law (1.1). One finds that, contrary to the expectation from the distribution of light, the rotation curve does not decline at larger distances from the center. *Like our own Galaxy, spiral galaxies contain a large amount of dark matter; the visible matter is embedded in a halo of dark matter.* We can only get rough estimates of the extent of this halo, but there are strong indications that it is substantially larger than the extent of the visual matter. For instance, the rotation curve is flat up to the largest radii where one still finds gas to measure the velocity. Studying dark matter in elliptical galaxies is more complicated, but the existence of dark halos has also been proven for ellipticals.

The Hertzsprung–Russell diagram of stars, or their color–magnitude diagram (see Appendix B), has turned out to be the most important diagram in stellar astrophysics. The fact that most stars are aligned along a one-dimensional sequence, the main sequence, led to the conclusion that, for main-sequence stars, the luminosity and the surface temperature are not independent parameters. Instead, the properties of such stars are in principle characterized by only a single parameter: the stellar mass. We will also see that the various properties of galaxies are not independent parameters. Rather, dynamical properties (such as the rotational velocity of spirals) are closely related to the luminosity. These scaling relations are of similar importance to the study of galaxies as the Hertzsprung–Russell diagram is for stars. In addition, they turn out to be very convenient tools for the determination of galaxy distances.

Like our Milky Way, other galaxies also seem to harbor a SMBH in their center. We obtained the astonishing result that the mass of such a SMBH is closely related to the velocity distribution of stars in elliptical galaxies or in the bulge of spirals. The physical reason for this close correlation is as yet unknown, but it strongly suggests a joint evolution of galaxies and their SMBHs.

1.2.3 The Hubble Expansion of the Universe

The radial velocity of galaxies, measured by means of the Doppler shift of spectral lines (Fig. 1.9), is positive for nearly all galaxies, i.e., they appear to be moving away from us. In 1928, Edwin Hubble discovered that

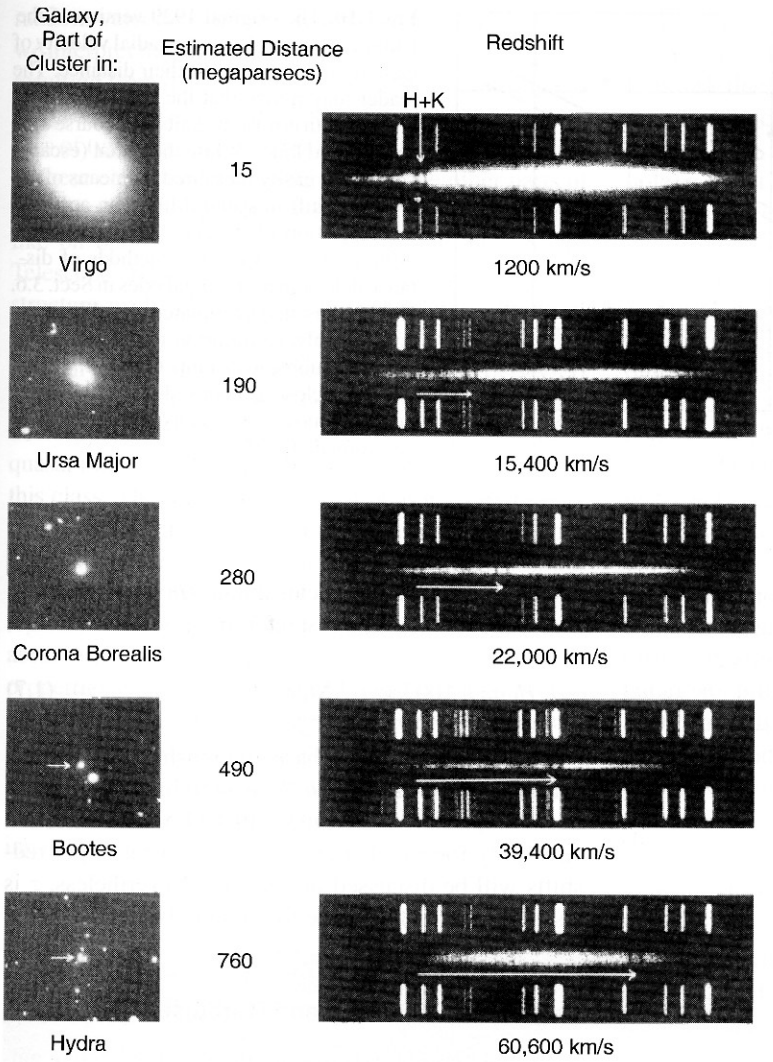

Fig. 1.9. The spectra of galaxies show characteristic spectral lines, e.g., the H + K lines of calcium. These lines, however, do not appear at the wavelengths measured in the laboratory but are in general shifted towards longer wavelengths. This is shown here for a set of sample galaxies, with distance increasing from top to bottom. The shift in the lines, interpreted as being due to the Doppler effect, allows us to determine the relative radial velocity – the larger it is, the more distant the galaxy is. The discrete lines above and below the spectra are for calibration purposes only

this escape velocity v increases with the distance of the galaxy. He identified a linear relation between the radial velocity v and the distance D of galaxies, called a Hubble law,

$$\boxed{v = H_0 D}\,, \tag{1.2}$$

where H_0 is a constant. If we plot the radial velocity of galaxies against their distance, as is done in the Hubble diagram of Fig. 1.10, the resulting points are approximated by a straight line, with the slope being determined by the constant of proportionality, H_0, which is called the *Hubble constant*. The fact that all galaxies seem to move away from us with a velocity which increases linearly with their distance is interpreted such that the Universe is expanding. We will see later that this *Hubble expansion* of the Universe is a natural property of cosmological world models.

The value of H_0 has been determined with appreciable precision only in recent years, yielding the conservative estimate

$$60\,\mathrm{km\,s^{-1}\,Mpc^{-1}} \lesssim H_0 \lesssim 80\,\mathrm{km\,s^{-1}\,Mpc^{-1}}\,, \tag{1.3}$$

obtained from several different methods which will be discussed later. The error margins vary for the differ-

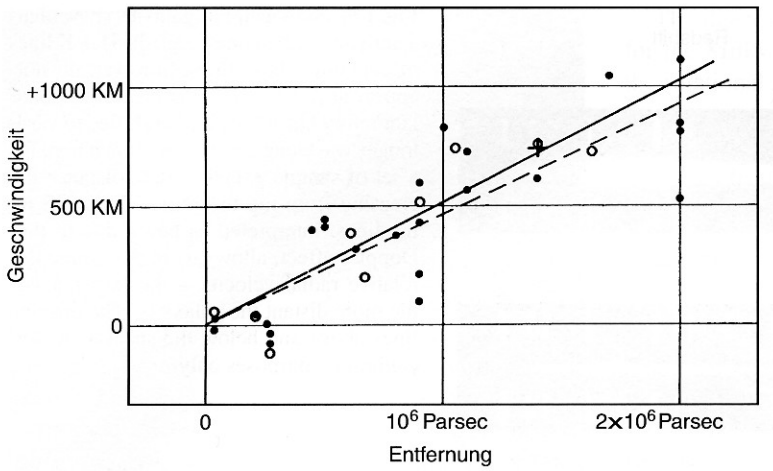

Fig. 1.10. The original 1929 version of the Hubble diagram shows the radial velocity of galaxies as a function of their distance. The reader may notice that the velocity axis is labeled with errornous units – of course they should read km/s. While the radial (escape) velocity is easily measured by means of the Doppler shift in spectral lines, an accurate determination of distances is much more difficult; we will discuss methods of distance determination for galaxies in Sect. 3.6. Hubble has underestimated the distances considerably, resulting in too high a value for the Hubble constant. Only very few and very close galaxies show a blueshift, i.e., they move towards us; one of these is Andromeda (= M31)

ent methods and also for different authors. The main problem in determining H_0 is in measuring the absolute distance of galaxies, whereas Doppler shifts are easily measurable. If one assumes (1.2) to be valid, the radial velocity of a galaxy is a measure of its distance. One defines the *redshift*, z, of an object from the wavelength shift in spectral lines,

$$z := \frac{\lambda_{\rm obs} - \lambda_0}{\lambda_0}\,, \quad \lambda_{\rm obs} = (1+z)\lambda_0\,, \tag{1.4}$$

with λ_0 denoting the wavelength of a spectral transition in the rest-frame of the emitter and $\lambda_{\rm obs}$ the observed wavelength. For instance, the Lyman-α transition, i.e., the transition from the first excited level to the ground state in the hydrogen atom is at $\lambda_0 = 1216$ Å. For small redshifts,

$$v \approx zc\,, \tag{1.5}$$

whereas this relation has to be modified for large redshifts, together with the interpretation of the redshift itself.[5] Combining (1.2) and (1.5), we obtain

$$D \approx \frac{zc}{H_0} \approx 3000\, z\, h^{-1}\,\mathrm{Mpc}\,, \tag{1.6}$$

where the uncertainty in determining H_0 is parametrized by the scaled Hubble constant h, defined as

$$\boxed{H_0 = h\,100\,\mathrm{km\,s^{-1}\,Mpc^{-1}}}\,. \tag{1.7}$$

Distance determinations based on redshift therefore always contain a factor of h^{-1}, as seen in (1.6). It needs to be emphasized once more that (1.5) and (1.6) are valid only for $z \ll 1$; the generalization for larger redshifts will be discussed in Sect. 4.3. Nevertheless, z is also a measure of distance for large redshifts.

1.2.4 Active Galaxies and Starburst Galaxies

A special class of galaxies are the so-called active galaxies which have a very strong energy source in their center (active galactic nucleus, AGN). The best-known representatives of these AGNs are the quasars, objects typically at high redshift and with quite exotic properties. Their spectrum shows strong emission lines which can be extremely broad, with a relative width of $\Delta\lambda/\lambda \sim 0.03$. The line width is caused by very high

[5] What is observed is the wavelength shift of spectral lines. Depending on the context, it is interpreted either as a radial velocity of a source moving away from us – for instance, if we measure the radial velocity of stars in the Milky Way – or as a cosmological escape velocity, as is the case for the Hubble law. It is in principle impossible to distinguish between these two interpretations, because a galaxy not only takes part in the cosmic expansion but it can, in addition, have a so-called peculiar velocity. We will therefore use the words "Doppler shift" and "redshift", respectively, and "radial velocity" depending on the context, but always keeping in mind that both are measured by the shift of spectral lines. Only when observing the distant Universe where the Doppler shift is fully dominated by the cosmic expansion will we exclusively call it "redshift".

random velocities of the gas which emits these line: if we interpret the line width as due to Doppler broadening resulting from the superposition of lines of emitting gas with a very broad velocity distribution, we obtain velocities of typically $\Delta v \sim 10\,000$ km/s. The central source of these objects is much brighter than the other parts of the galaxy, making these sources appear nearly point-like on optical images. Only with the Hubble Space Telescope (HST) did astronomers succeed in detecting structure in the optical emission for a large sample of quasars (Fig. 1.11).

Many properties of quasars resemble those of Seyfert type I galaxies, which are galaxies with a very luminous nucleus and very broad emission lines. For this reason, quasars are often interpreted as extreme members of this class. The total luminosity of quasars is extremely large, with some of them emitting more than a thousand times the luminosity of our Galaxy. In addition, this radiation must originate from a very small spatial region whose size can be estimated, e.g., from the variability time-scale of the source. Due to these and other properties which will be discussed in Chap. 5, it is concluded that the nuclei of active galaxies must contain a supermassive black hole as the central powerhouse. The radiation is produced by matter falling towards this black hole, a process called accretion, thereby converting its gravitational potential energy into kinetic energy. If this kinetic energy is then transformed into internal energy (i.e., heat) as happens in the so-called accretion disk due to friction, it can get radiated away. This is in fact an extremely efficient process of energy production. For a given mass, the accretion onto a black hole is about 10 times more efficient than the nuclear fusion of hydrogen into helium. AGNs often emit radiation across a very large portion of the electromagnetic spectrum, from radio up to X-ray and gamma radiation.

Spiral galaxies still form stars today; indeed star formation is a common phenomenon in galaxies. In addition, there are galaxies with a considerably higher star-formation rate than "normal" spirals. These galaxies are undergoing a burst of star formation and are thus known as *starburst galaxies*. Their star-formation rates are typically between 10 and 300 $M_\odot$/yr, whereas our Milky Way gives birth to about 2 $M_\odot$/yr of new stars. This vigorous star formation often takes place in localized regions, e.g., in the vicinity of the center of the respective galaxy. Starbursts are substantially affected, if not triggered, by disturbances in the gravitational field of the galaxy, such as those caused by galaxy interactions. Such starburst galaxies (see Fig. 1.12) are extremely luminous in the far-infrared (FIR); they emit up to 98% of their total luminosity in this part of the spectrum. This happens by dust emission: dust in these galaxies absorbs a large proportion of the energetic UV radiation

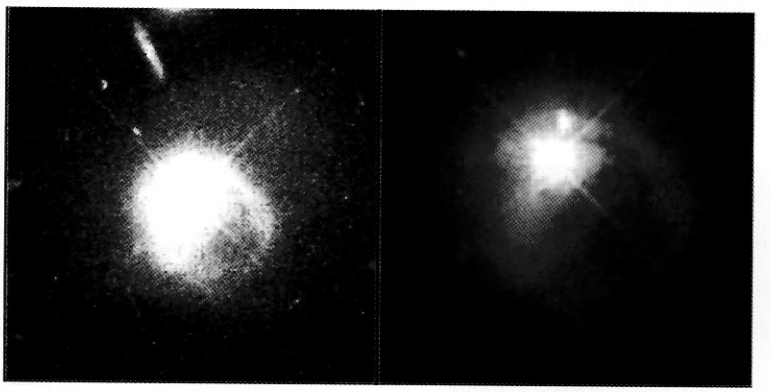

Fig. 1.11. The quasar PKS 2349 is located at the center of a galaxy, its host galaxy. The diffraction spikes (diffraction patterns caused by the suspension of the telescope's secondary mirror) in the middle of the object show that the center of the galaxy contains a point source, the actual quasar, which is significantly brighter than its host galaxy. The galaxy shows clear signs of distortion, visible as large and thin tidal tails. The tails are caused by a neighboring galaxy that is visible in the right-hand image, just above the quasar; it is about the size of the Large Magellanic Cloud. Quasar host galaxies are often distorted or in the process of merging with other galaxies. The two images shown here differ in their brightness contrast

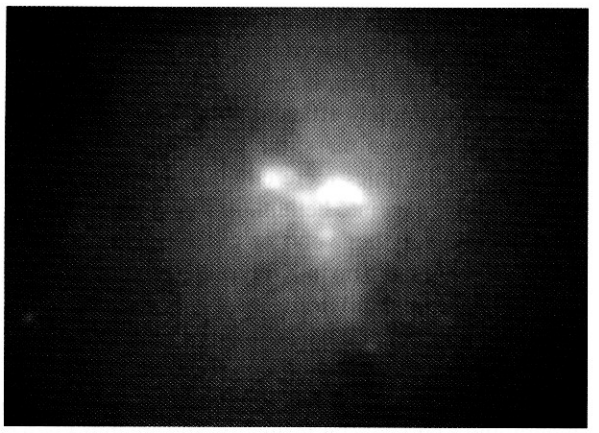

Fig. 1.12. Arp 220 is the most luminous object in the local Universe. Originally cataloged as a peculiar galaxy, the infrared satellite IRAS later discovered its enormous luminosity in the infrared (IR). Arp 220 is the prototype of ultra-luminous infrared galaxies (ULIRGs). This near-IR image taken with the Hubble Space Telescope (HST) unveils the structure of this object. With two colliding spiral galaxies in the center of Arp 220, the disturbances in the interstellar medium caused by this collision trigger a starburst. Dust in the galaxy absorbs most of the ultraviolet (UV) radiation from the young hot stars and re-emits it in the IR

produced in the star-formation region and then re-emits this energy in the form of thermal radiation in the FIR.

1.2.5 Voids, Clusters of Galaxies, and Dark Matter

The likelihood of galaxies interacting (Fig. 1.13) is enhanced by the fact that galaxies are not randomly distributed in space. The projection of galaxies on the celestrial sphere, for instance, shows a distinct structure. In addition, measuring the distances of galaxies allows a determination of their three-dimensional distribution. One finds a strong correlation of the galaxy positions. There are regions in space that have a very high galaxy density, but also regions where nearly no galaxies are seen at all. The latter are called *voids*. Such voids can have diameters of up to $30\,h^{-1}$ Mpc.

Clusters of galaxies are gravitationally bound systems of a hundred or more galaxies in a volume of diameter $\sim 2\,h^{-1}$ Mpc. Clusters predominantly contain early-type galaxies, so there is not much star formation taking place any more. Some clusters of galaxies seem to be circular in projection, others have a highly elliptical or irregular distribution of galaxies; some even have more than one center. The cluster of galaxies closest to us is the Virgo Cluster, at a distance of ~ 18 Mpc; it is a cluster with an irregular galaxy distribution. The closest regular cluster is Coma, at a distance of ~ 90 Mpc.[6] Coma (Fig. 1.14) contains about 1000 luminous galaxies, of which 85% are early-type galaxies.

[6]The distances of these two clusters are not determined from redshift measurements, but by direct methods that will be discussed in Sect. 3.6; such direct measurements are one of the most successful methods of determining the Hubble constant.

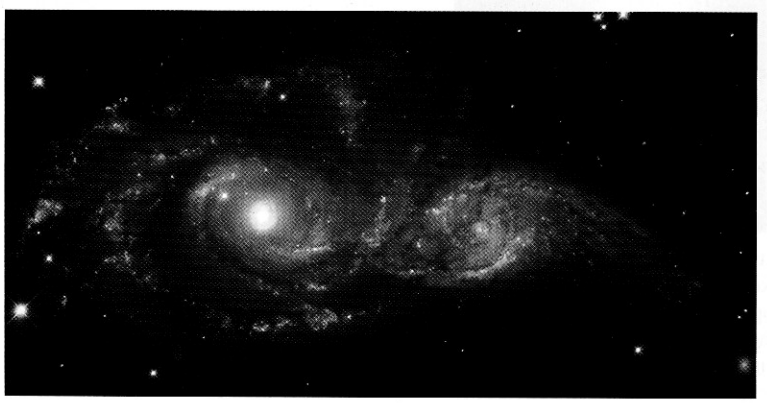

Fig. 1.13. Two spiral galaxies interacting with each other. NGC 2207 (on the left) and IC 2163 are not only close neighbors in projection: the strong gravitational tidal interaction they are exerting on each other is clearly visible in the pronounced tidal arms, particularly visible to the right of the right-hand galaxy. Furthermore, a bridge of stars is seen to connect these two galaxies, also due to tidal gravitational forces. This image was taken with the Hubble Space Telescope

Fig. 1.14. The Coma cluster of galaxies, at a distance of roughly 90 Mpc from us, is the closest massive regular cluster of galaxies. Almost all objects visible in this image are galaxies associated with the cluster – Coma contains more than a thousand luminous galaxies

In 1933, Fritz Zwicky measured the radial velocities of the galaxies in Coma and found that they have a dispersion of about 1000 km/s. From the total luminosity of all its galaxies the mass of the cluster can be estimated. If the stars in the cluster galaxies have an average mass-to-light ratio (M/L) similar to that of our Sun, we would conclude $M = (M_\odot/L_\odot)L$. However, stars in early-type galaxies are on average slightly less massive than the Sun and thus have a slightly higher M/L.[7] Thus, the above mass estimate needs to be increased by a factor of ~ 10.

Zwicky then estimated the mass of the cluster by multiplying the luminosity of its member galaxies with the mass-to-light ratio. From this mass and the size of the cluster, he could then estimate the velocity that a galaxy needs to have in order to escape from the gravitational field of the cluster – the escape velocity. He found that the characteristic peculiar velocity of cluster galaxies (i.e., the velocity relative to the mean velocity) is substantially larger than this escape velocity. In this case, the galaxies of the cluster would fly apart on a time-scale of about 10^9 years – the time it takes a galaxy to cross through the cluster once – and, consequently, the cluster would dissolve. However, since Coma seems to be a relaxed cluster, i.e., it is in equilibrium and thus its age is definitely larger than the dynamical time-scale of 10^9 years, Zwicky concluded that the Coma cluster contains significantly more mass than the sum of the masses of its galaxies. Using the virial theorem[8] he was able to estimate the mass of the cluster from the velocity distribution of the galaxies. This was the first clear indicator of the existence of dark matter.

X-ray satellites later revealed that clusters of galaxies are strong sources of X-ray radiation. They contain hot gas, with temperatures ranging from 10^7 K up to 10^8 K (Fig. 1.15). This gas temperature is another measure for the depth of the cluster's potential well, since the hotter the gas is, the deeper the potential well has to be to prevent the gas from escaping via evaporation. Mass estimates based on the X-ray temperature result in values that are comparable to those from the velocity dispersion of the cluster galaxies, clearly confirming the hypothesis of the existence of dark matter in clusters. A third method for determining cluster masses, the so-called gravitational lensing effect, utilizes the fact that light is deflected in a gravitational field. The angle through which light rays are bent due to the presence of a massive object depends on the mass of that object. From observation and analysis of the gravitational lensing effect in clusters of galaxies, cluster masses are derived that are in agreement with those from the two other methods. Therefore, clusters of galaxies are a second class of cosmic objects whose mass is dominated by dark matter.

Clusters of galaxies are cosmologically young structures. Their dynamical time-scale, i.e., the time in which the mass distribution in a cluster settles into an equilibrium state, is estimated as the time it takes a member galaxy to fully cross the cluster once. With a characteristic velocity of $v \sim 1000$ km/s and a diameter of $2R \sim 2$ Mpc one thus finds

$$t_{\rm dyn} \sim \frac{2R}{v} \sim 2 \times 10^9 \ {\rm yr} \, . \qquad (1.9)$$

[7] In Chap. 3 we will see that for stars in spiral galaxies $M/L \sim 3 M_\odot/L_\odot$ on average, while for those in elliptical galaxies a larger value of $M/L \sim 10\, M_\odot/L_\odot$ applies. Here and throughout this book, mass-to-light ratios are quoted in Solar units.

[8] The virial theorem in its simplest form says that, for an isolated dynamical system in a stationary state of equilibrium, the kinetic energy is just half the potential energy,

$$E_{\rm kin} = \frac{1}{2}|E_{\rm pot}| \, . \qquad (1.8)$$

In particular, the system's total energy is $E_{\rm tot} = E_{\rm kin} + E_{\rm pot} = E_{\rm pot}/2 = -E_{\rm kin}$.

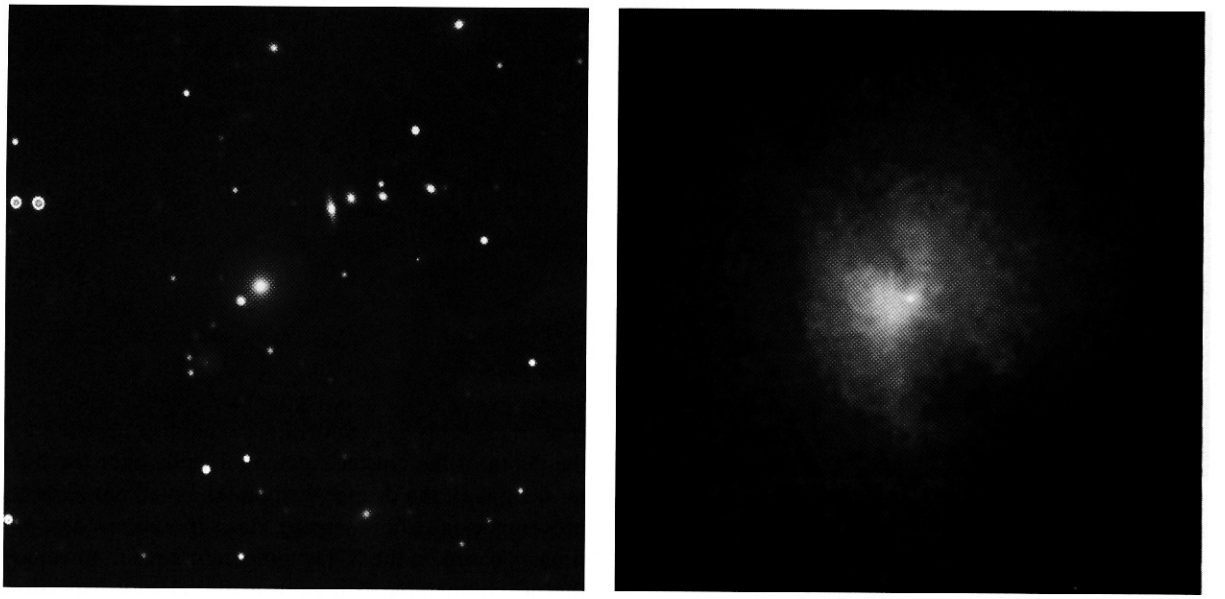

Fig. 1.15. The Hydra A cluster of galaxies. The left-hand figure shows an optical image, the one on the right an image taken with the X-ray satellite Chandra. The cluster has a redshift of $z \approx 0.054$ and is thus located at a distance of about 250 Mpc. The X-ray emission originates from gas at a temperature of 40×10^6 K which fills the space between the cluster galaxies. In the center of the cluster, the gas is cooler by about 15%

As we will later see, the Universe is about 14×10^9 years old. During this time galaxies have not had a chance to cross the cluster many times. Therefore, clusters still contain, at least in principle, information about their initial state. Most clusters have not had the time to fully relax and evolve into a state of equilibrium that would be largely independent of their initial conditions. Comparing this with the time taken for the Sun to rotate around the center of the Milky Way – about 2×10^8 years – galaxies thus have had plenty of time to reach their state of equilibrium.

Besides massive clusters of galaxies there are also galaxy groups, which sometimes contain only a few luminous galaxies. Our Milky Way is part of such a group, the Local Group, which also contains M31 (Andromeda) which is another dominant galaxy, as well as some far less luminous galaxies such as the Magellanic Clouds. Some groups of galaxies are very compact, i.e., their galaxies are confined within a very small volume (Fig. 1.16). Interactions between these galaxies cause the lifetimes of many such groups to be much smaller than the age of the Universe, and the galaxies in such groups will merge.

1.2.6 World Models and the Thermal History of the Universe

Quasars, clusters of galaxies, and nowadays even single galaxies are also found at very high redshifts where the simple Hubble law (1.2) is no longer valid. It is therefore necessary to generalize the distance–redshift relation. This requires considering world models as a whole, which are also called cosmological models. The dominant force in the Universe is gravitation. On the one hand, weak and strong interactions both have an extremely small (subatomic) range, and on the other hand, electromagnetic interactions do not play a role on large scales since the matter in the Universe is on average electrically neutral. Indeed, if it was not, currents would immediately flow to balance net charge densities. The accepted theory of gravitation is the theory of General Relativity (GR), formulated by Albert Einstein in 1915.

Based on the two postulates that (1) our place in the Universe is not distinguished from other locations and that (2) the distribution of matter around us is isotropic, at least on large scales, one can construct

Fig. 1.16. The galaxy group HCG87 belongs to the class of so-called compact groups. In this HST image we can see three massive galaxies belonging to this group: an edge-on spiral in the lower part of the image, an elliptical galaxy to the lower right, and another spiral in the upper part. The small spiral in the center is a background object and therefore does not belong to the group. The two lower galaxies have an active galactic nucleus, whereas the upper spiral seems to be undergoing a phase of star formation. The galaxies in this group are so close together that in projection they appear to touch. Between the galaxies, gas streams can be detected. The galaxies are disturbing each other, which could be the cause of the nuclear activity and star formation. The galaxies are bound in a common gravitational potential and will heavily interfere and presumably merge on a cosmologically small time-scale, which means in only a few orbits, with an orbit taking about 10^8 years. Such merging processes are of utmost importance for the evolution of the galaxy population

homogeneous and isotropic world models (so-called Friedmann–Lemaître models) that obey the laws of General Relativity. Expanding world models that contain the Hubble expansion result from this theory naturally. Essentially, these models are characterized by three parameters:

- the current expansion rate of the Universe, i.e., the Hubble constant H_0;
- the current mean matter density of the Universe ρ_m, often parametrized by the dimensionless *density parameter*

$$\Omega_\mathrm{m} = \frac{8\pi G}{3H_0^2}\rho_\mathrm{m}\,; \tag{1.10}$$

- and the density of the so-called vacuum energy, described by the cosmological constant Λ or by the corresponding density parameter of the vacuum

$$\Omega_\Lambda = \frac{\Lambda}{3H_0^2}\,. \tag{1.11}$$

The cosmological constant was originally introduced by Einstein to allow stationary world models within GR. After the discovery of the Hubble expansion he called the introduction of Λ into his equations his greatest blunder. In quantum mechanics Λ attains a different interpretation, that of an energy density of the vacuum.

The values of the cosmological parameters are known quite accurately today (see Chap. 8), with values of $\Omega_\mathrm{m} \approx 0.3$ and $\Omega_\Lambda \approx 0.7$. The discovery of a non-vanishing Ω_Λ came completely unexpectedly. To date, all attempts have failed to compute a reasonable value for Ω_Λ from quantum mechanics. By that we mean a value which has the same order-of-magnitude as the one we derive from cosmological observations. In fact, simple and plausible estimates lead to a value of Λ that is $\sim 10^{120}$ times larger than that obtained from observation, a tremendously bad estimate indeed. This huge discrepancy is probably one of the biggest challenges in fundamental physics today.

According to the Friedmann–Lemaître models, the Universe used to be smaller and hotter in the past, and it has continuously cooled down in the course of expansion. We are able to trace back the cosmic expansion under the assumption that the known laws of physics were also valid in the past. From that we get the Big Bang model of the Universe, according to which our Universe has evolved out of a very dense and very hot state, the so-called *Big Bang*. This world model makes a number of predictions that have been verified convincingly:

1. About 1/4 of the baryonic matter in the Universe should consist of helium which formed about 3 min after the Big Bang, while most of the rest consists

of hydrogen. This is indeed the case: the mass fraction of helium in metal-poor objects, whose chemical composition has not been significantly modified by processes of stellar evolution, is about 24%.

2. From the exact fraction of helium one can derive the number of neutrino families – the more neutrino species that exist, the larger the fraction of helium will be. From this, it was derived in 1981 that there are 3 kinds of neutrinos. This result was later confirmed by particle accelerator experiments.
3. Thermal radiation from the hot early phase of the Universe should still be measurable today. Predicted in 1946 by George Gamow, it was discovered by Arno Penzias and Robert Wilson in 1965. The corresponding photons have propagated freely after the Universe cooled down to about 3000 K and the plasma constituents combined to neutral atoms, an epoch called recombination. As a result of cosmic expansion, this radiation has cooled down to about $T_0 \approx 2.73$ K. This microwave radiation is nearly perfectly isotropic, once we subtract the radiation which is emitted locally by the Milky Way (see Fig. 1.17). Indeed, measurements from the COBE satellite showed that the cosmic microwave background (CMB) is the most accurate blackbody spectrum ever measured.
4. Today's structures in the Universe have evolved out of very small density fluctuations in the early cosmos. The seeds of structure formation must have already been present in the early phases of cosmic evolution. These density fluctuations should also be visible as small temperature fluctuations in the microwave background emitted about 380 000 years after the Big Bang at the epoch of recombination. In fact, COBE was the first to observe these predicted anisotropies (see Fig. 1.17). Later experiments, especially the WMAP satellite, observed the structure of the microwave background at much improved angular resolution and verified the theory of structure formation in the Universe in detail (see Sect. 8.6).

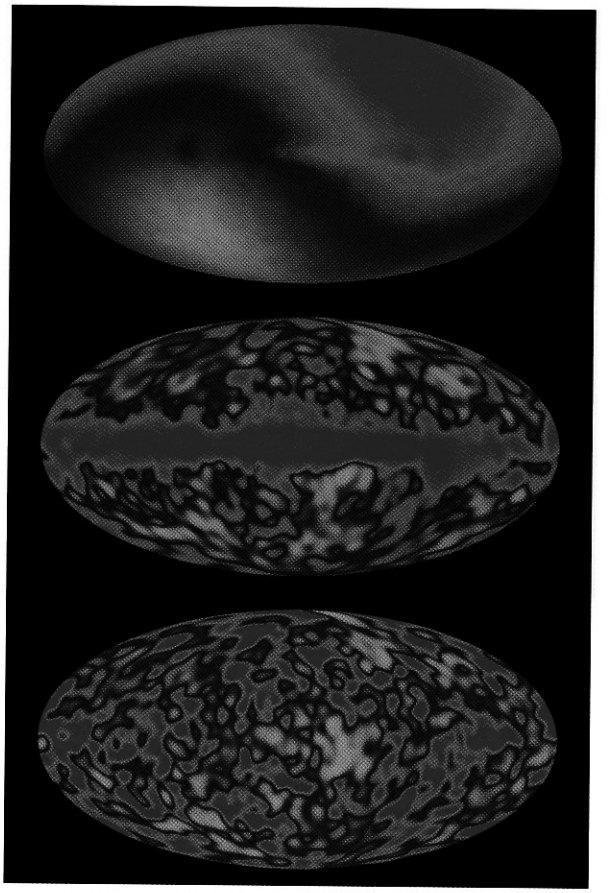

Fig. 1.17. Temperature distribution of the cosmic microwave background on the sky as measured by the COBE satellite. The uppermost image shows a dipole distribution; it originates from the Earth's motion relative to the rest-frame of the CMB. We move at a speed of ~ 600 km/s relative to that system, which leads to a dipole anisotropy with an amplitude of $\Delta T/T \sim v/c \sim 2 \times 10^{-3}$ due to the Doppler effect. If this dipole contribution is subtracted, we get the map in the middle which clearly shows the emission from the Galactic disk. Since this emission has a different spectral energy distribution (it is not a blackbody of $T \sim 3$ K), it can also be subtracted to get the temperature map at the bottom. These are the primordial fluctuations of the CMB, with an amplitude of about $\Delta T/T \sim 2 \times 10^{-5}$

With these predictions so impressively confirmed, in this book we will exclusively consider this cosmological model; currently there is no competing model of the Universe that could explain these very basic cosmological observations in such a natural way. In addition, this model does not seem to contradict any fundamental observation in cosmology. However, as the existence of a non-vanishing vacuum energy density shows, together with a matter density ρ_m that is about six times the mean baryon density in the Universe (which can be derived from the abundance of the chemical elements formed in the Big Bang), the physical nature of about 95% of the content of our Universe is not yet understood.

The CMB photons we receive today had their last physical interaction with matter when the Universe was about 3.8×10^5 years old. Also, the most distant galaxies and quasars known today (at $z \sim 6.5$) are strikingly young – we see them at a time when the Universe was less than a tenth of its current age. The exact relation between the age of the Universe at the time of the light emission and the redshift depends on the cosmological parameters H_0, Ω_m, and Ω_Λ. In the special case that $\Omega_\mathrm{m} = 1$ and $\Omega_\Lambda = 0$, called the *Einstein–de Sitter model*, one obtains

$$t(z) = \frac{2}{3H_0} \frac{1}{(1+z)^{3/2}} \,. \tag{1.12}$$

In particular, the age of the Universe today (i.e., at $z = 0$) is, according to this model,

$$t_0 = \frac{2}{3H_0} \approx 6.5 \times 10^9 \, h^{-1} \,\mathrm{yr} \,. \tag{1.13}$$

The Einstein–de Sitter (EdS) model is the simplest world model and we will sometimes use it as a reference, but recent observations suggest that $\Omega_\mathrm{m} < 1$ and $\Omega_\Lambda > 0$. The mean density of the Universe in the EdS model is

$$\rho_0 = \rho_\mathrm{cr} \equiv \frac{3H_0^2}{8\pi G} \approx 1.9 \times 10^{-29} \, h^2 \,\mathrm{g\,cm^{-3}} \,, \tag{1.14}$$

hence it is really, really small.

1.2.7 Structure Formation and Galaxy Evolution

The low amplitude of the CMB anisotropies implies that the inhomogeneities must have been very small at the epoch of recombination, whereas today's Universe features very large density fluctuations, at least on scales of clusters of galaxies. Hence, the density field of the cosmic matter must have evolved. This structure evolution occurs because of gravitational instability, in that an overdense region will expand more slowly than the mean Universe due to its self-gravity. Therefore, any relative overdensity becomes amplified in time. The growth of density fluctuations in time will then cause the formation of large-scale structures, and the gravitational instability is also responsible for the formation of galaxies and clusters. Our world model sketched above predicts the abundance of galaxy clusters as a function of redshift, which can be compared with the observed cluster counts. This comparison can then be used to determine cosmological parameters.

Another essential conclusion from the smallness of the CMB anisotropies is the existence of dark matter on cosmic scales. The major fraction of cosmic matter is dark matter. The baryonic contribution to the matter density is $\lesssim 20\%$ and to the total energy density $\lesssim 5\%$. The energy density of the Universe is dominated by the vacuum energy.

Unfortunately, the spatial distribution of dark matter on large scales is not directly observable. We only observe galaxies or, more precisely, their stars and gas. One might expect that galaxies would be located preferentially where the dark matter density is high. However, it is by no means clear that local fluctuations of the galaxy number density are strictly proportional to the density of dark matter. The relation between the dark and luminous matter distributions is currently only approximately understood.

Eventually, this relation has to result from a detailed understanding of galaxy formation and evolution. Locations with a high density of dark matter can support the formation of galaxies. Thus we will have to examine how galaxies form and why there are different kinds of galaxies. In other words, what decides whether a forming galaxy will become an elliptical or a spiral? This question has not been definitively answered yet, but it is supposed that ellipticals can form only by the merging of galaxies. Indeed, the standard model of the Universe predicts that small galaxies will form first; larger galaxies will be formed later through the ongoing merger of smaller ones.

The evolution of galaxies can actually be observed directly. Galaxies at high redshift (i.e., cosmologically young galaxies) are in general smaller and bluer, and the star-formation rate was significantly higher in the earlier Universe than it is today. The change in the mean color of galaxies as a function of redshift can be understood as a combination of changes in the star formation processes and an aging of the stellar population.

1.2.8 Cosmology as a Triumph of the Human Mind

Cosmology, extragalactic astronomy, and astrophysics as a whole are a heroic undertaking of the human mind and a triumph of physics. To understand the Universe we

apply physical laws that were found empirically under completely different circumstances. All the known laws of physics were derived "today" and, except for General Relativity, are based on experiments on a laboratory scale or, at most, on observations in the Solar System, such as Kepler's laws which formed the foundation for the Newtonian theory of gravitation. Is there any a priori reason to assume that these laws are also valid in other regions of the Universe or at completely different times? However, this is apparently indeed the case: nuclear reactions in the early Universe seem to obey the same laws of strong interaction that are measured today in our laboratories, since otherwise the prediction of a 25% mass fraction of helium would not be possible. Quantum mechanics, describing the wavelengths of atomic transitions, also seems to be valid at very large distances – since even the most distant objects show emission lines in their spectra with frequency ratios (which are described by the laws of quantum mechanics) identical to those in nearby objects.

By far the greatest achievement is General Relativity. It was originally formulated by Albert Einstein since his Special Theory of Relativity did not allow him to incorporate Newtonian gravitation. No empirical findings were known at that time (1915) which would not have been explained by the Newtonian theory of gravity. Nevertheless, Einstein developed a totally new theory of gravitation for purely theoretical reasons. The first success of this theory was the correct description of the gravitational deflection of light by the Sun, measured in 1919, and of the perihelion rotation of Mercury.[9] His theory permits a description of the expanding Universe, which became necessary after Hubble's discovery in 1928. Only with the help of this theory can we reconstruct the history of the Universe back into the past. Today this history seems to be well understood up to the time when the Universe was about 10^{-6} s old and had a temperature of about 10^{13} K. Particle physics models allow an extrapolation to even earlier epochs.

The cosmological predictions discussed above are based on General Relativity describing an expanding Universe, therefore providing a test of Einstein's theory. On the other hand, General Relativity also describes much smaller systems and with much stronger gravitational fields, such as neutron stars and black holes. With the discovery of a binary system consisting of two neutron stars, the binary pulsar PSR 1913+16, in the last ~ 25 years very accurate tests of General Relativity have become possible. For example, the observed perihelion rotation in this binary system and the shrinking of the binary orbit over time due to the radiation of energy by gravitational waves is very accurately described by General Relativity. Together, General Relativity has been successfully tested on length-scales from 10^{11} cm (the characteristic scale of the binary pulsar) to 10^{28} cm (the size of the visible Universe), that is over more than 10^{17} orders of magnitude – an impressive result indeed!

[9]This was already known in 1915, but it was not clear whether it might not have any other explanation, e.g., a quadrupole moment of the mass distribution of the Sun.

1.3 The Tools of Extragalactic Astronomy

Extragalactic sources – galaxies, quasars, clusters of galaxies – are at large distances. This means that in general they appear to be faint even if they are intrinsically luminous. They are also seen to have a very small angular size despite their possibly large linear extent. In fact, just three extragalactic sources are visible to the naked eye: the Andromeda galaxy (M31) and the Large and Small Magellanic Clouds. Thus for extragalactic astronomy, telescopes are needed that have large apertures (photon collecting area) and a high angular resolution. This applies to all wavebands, from radio astronomy to gamma ray astronomy.

The properties of astronomical telescopes and their instruments can be judged by different criteria, and we will briefly describe the most important ones. The *sensitivity* specifies how dim a source can be and still be observable in a given integration time. The sensitivity depends on the aperture of the telescope as well as on the efficiency of the instrument and the sensitivity of the detector. The sensitivity of optical telescopes, for instance, was increased by a large factor when CCDs replaced photographic plates as detectors in the early 1980s. The sensitivity also depends on the sky background, i.e., the brightness of the sky caused by non-astronomical sources. Artificial light in inhabited regions has forced optical telescopes to retreat into more and more remote areas of the world where *light pollution* is minimized. Radio astronomers have similar problems caused by radio emission from the telecommunication infrastructure

of modern civilization. The *angular resolution* of a telescope specifies down to which angular separation two sources in the sky can still be separated by the detector. For diffraction-limited observations like those made with radio telescopes or space-born telescopes, the angular resolution $\Delta\theta$ is limited by the diameter D of the telescope. For a wavelength λ one has $\Delta\theta = \lambda/D$. For optical and near-infrared observations from the ground, the angular resolution is in general limited by turbulence in the atmosphere, which explains the choice of high mountain tops as sites for optical telescopes. These atmospheric turbulences cause, due to scintillation, the smearing of the images of astronomical sources, an effect that is called *seeing*. In interferometry, where one combines radiation detected by several telescopes, the angular resolution is limited by the spatial separation of the telescopes. The *spectral resolution* of an instrument specifies its capability to separate different wavelengths. The *throughput* of a telescope/instrument system is of particular importance in large sky surveys. For instance, the efficiency of photometric surveys depends on the number of spectra that can be observed simultaneously. Special multiplex spectrographs have been constructed for such tasks. Likewise, the efficiency of photometric surveys depends on the region of sky that can be observed simultaneously, i.e., the field-of-view of the camera. Finally, the efficiency of observations also depends on factors like the number of clear nights at an astronomical site, the fraction of an observing night in which actual science data is taken, the fraction of time an instrument cannot be used due to technical problems, the stability of the instrumental set-up (which determines the time required for calibration measurements), and many other such aspects.

In the rest of this section some telescopes will be presented that are of special relevance to extragalactic astronomy and to which we will frequently refer throughout the course of this book.

1.3.1 Radio Telescopes

With the exception of optical wavelengths, the Earth's atmosphere is transparent only for very large wavelengths – radio waves. The radio window of the atmosphere is cut off towards lower frequencies, at about $\nu \sim 10$ MHz, because radiation of a wavelength larger than $\lambda \sim 30$ m is reflected by the Earth's ionosphere and therefore cannot reach the ground. Below $\lambda \sim 5$ mm radiation is increasingly absorbed by oxygen and water vapor in the atmosphere. Therefore, below about $\lambda \sim 0.3$ mm ground-based observations are no longer possible.

Mankind became aware of cosmic radio radiation – in the early 1930s – only when noise in radio antennae was found that would not vanish, no matter how quiet the device was made. In order to identify the source of this noise the AT&T Bell Labs hired Karl Jansky, who constructed a movable antenna called "Jansky's Merry-Go-Round" (Fig. 1.18).

After some months Jansky had identified, besides thunderstorms, one source of interference that rose and set every day. However, it did not follow the course of the Sun which was originally suspected to be the source. Rather, it followed the stars. Jansky finally discovered that the signal originated from the direction of the center of the Milky Way. He published his result in 1933, but this publication also marked the end of his career as the world's first radio astronomer.

Inspired by Jansky's discovery, Grote Reber was the first to carry out real astronomy with radio waves. When AT&T refused to employ him, he built his own radio "dish" in his garden, with a diameter of nearly 10 m. Between 1938 and 1943, Reber compiled the first sky maps in the radio domain. Besides strong radiation from the center of the Milky Way he also identified sources in Cygnus and in Cassiopeia. Through Reber's research and publications radio astronomy became an accepted field of science after World War II.

The largest single-dish radio telescope is the Arecibo telescope, shown in Fig. 1.19. Due to its enormous area, and thus high sensitivity, this telescope, among other achievements, detected the first pulsar in a binary system, which is used as an important test laboratory for General Relativity (see Sect. 7.7). Also, the first extrasolar planet, in orbit around a pulsar, was discovered with the Arecibo telescope. For extragalactic astronomy Arecibo plays an important role in measuring the redshifts and line widths of spiral galaxies, both determined from the 21-cm emission line of neutral hydrogen (see Sect. 3.4).

The Effelsberg 100-m radio telescope of the Max-Planck-Institut für Radioastronomie was, for many years, the world's largest fully steerable radio telescope, but since 2000 this title has been claimed by the new

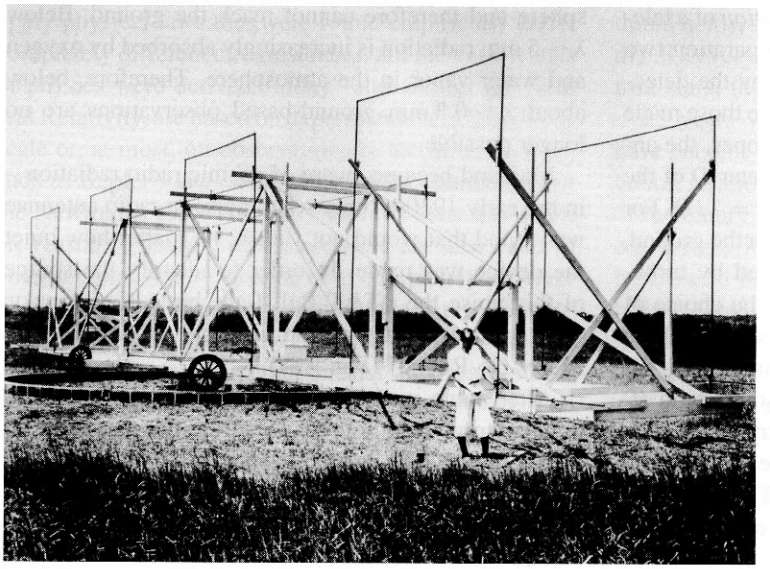

Fig. 1.18. "Jansky's Merry-Go-Round". By turning the structure in an azimuthal direction, a rough estimate of the position of radio sources could be obtained

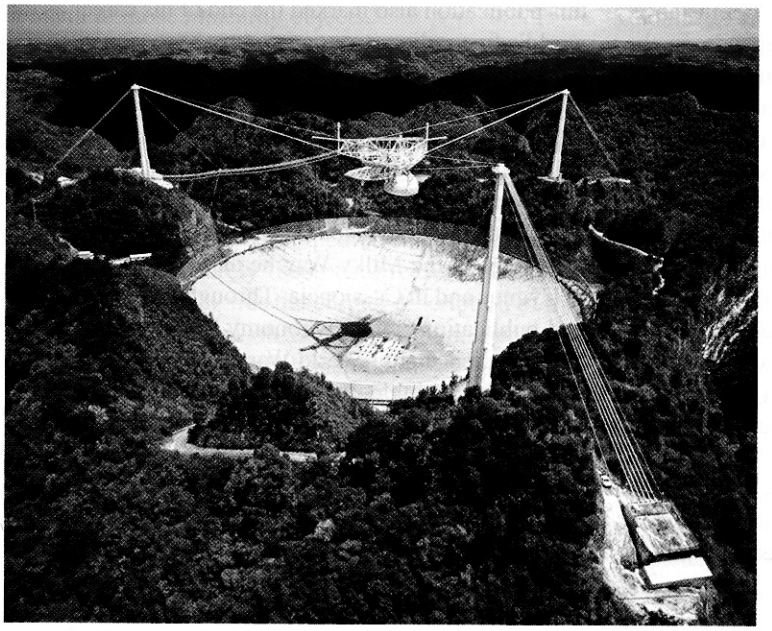

Fig. 1.19. With a diameter of 305 m, the Arecibo telescope in Puerto Rico is the largest single-dish telescope in the world; it may also be known from the James Bond movie "Goldeneye". The disadvantage of its construction is its lack of steerability. Tracking of sources is only possible within narrow limits by moving the secondary mirror

Green Bank Telescope (see Fig. 1.20) after the old one collapsed in 1988. With Effelsberg, for example, star-formation regions can be investigated. Using molecular line spectroscopy, one can measure their densities and temperatures. Magnetic fields also play a role in star formation, though many details still need to be clarified. By measuring the polarized radio flux, Effelsberg has mapped the magnetic fields of numerous spiral galaxies. In addition, due to its huge collecting area Effelsberg plays an important role in interferometry at very long baselines (see below).

Because of the long wavelength, the angular resolution of even large radio telescopes is fairly low, compared to optical telescopes. For this reason, radio

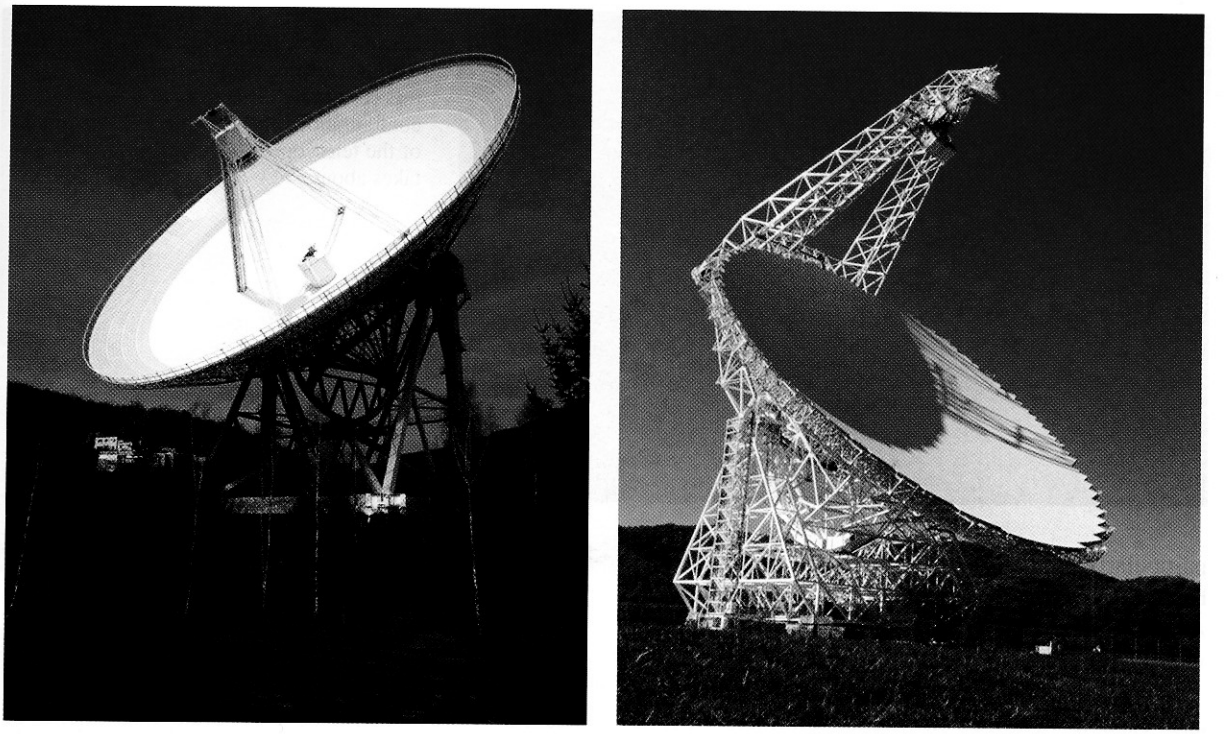

Fig. 1.20. The world's two largest fully steerable radio telescopes. Left: The 100-m telescope in Effelsberg. It was commissioned in 1972 and is used in the wavelength range from 3.5 mm to 35 cm. Eighteen different detector systems are necessary for this. Right: The Green Bank Telescope. It does not have a rotationally symmetric mirror; one axis has a diameter of 100 m and the other 110 m

astronomers soon began utilizing interferometric methods, where the signals obtained by several telescopes are correlated to get an interference pattern. One can then reconstruct the structure of the source from this pattern using Fourier transformation. With this method one gets the same resolution as one would achieve with a single telescope of a diameter corresponding to the maximum pair separation of the individual telescopes used.

Following the first interferometric measurements in England (around 1960) and the construction of the large Westerbork Synthesis Radio Telescope in the Netherlands (around 1970), at the end of the 1970s the Very Large Array (VLA) in New Mexico (see Fig. 1.21) began operating. With the VLA one achieved an angular resolution in the radio domain comparable to that of optical telescopes at that time. For the first time, this allowed the combination of radio and optical images with the same resolution and thus the study of cosmic sources over a range of several clearly separated wavelength regimes. With the advent of the VLA radio astronomy experienced an enormous breakthrough, particularly in the study of AGNs. It became possible to examine the large extended jets of quasars and radio galaxies in detail (see Sect. 5.1.2). Other radio interferometers must also be mentioned here, such as the British MERLIN, where seven telescopes with a maximum separation of 230 km are combined.

In the radio domain it is also possible to interconnect completely independent and diverse antennae to form an interferometer. For example, in Very Long Baseline Interferometry (VLBI) radio telescopes on different continents are used simultaneously. These frequently also include Effelsberg and the VLA. In 1995 a system of ten identical 25-m antennae was set up in the USA, exclusively to be used in VLBI, the Very Long Baseline Array (VLBA). Angular resolutions of better than a milliarcsecond (mas) can be achieved with VLBI. Therefore, in extragalactic astronomy VLBI is

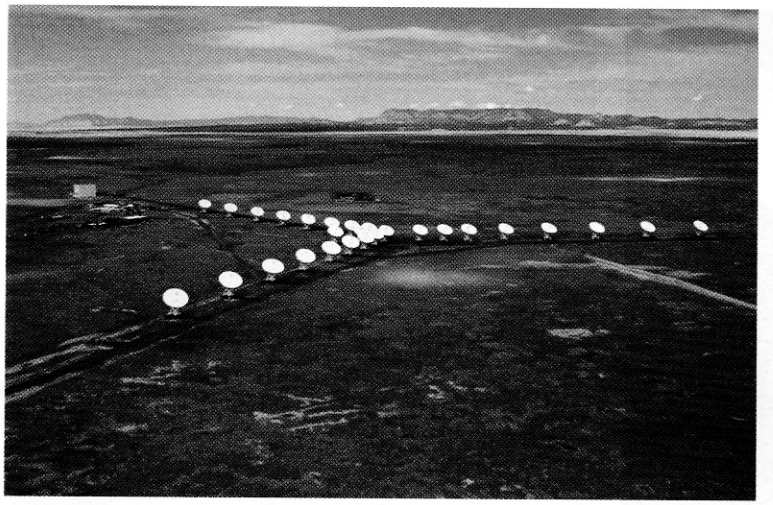

Fig. 1.21. The Very Large Array (VLA) in New Mexico consists of 27 antennae with a diameter of 25 m each that can be moved on rails. It is used in four different configurations that vary in the separation of the telescopes; switching configurations takes about two weeks

particularly used in the study of AGNs. With VLBI we have learned a great deal about the central regions of AGNs, such as the occurrence of apparent superluminal velocities in these sources.

Some of the radio telescopes described above are also capable of observing in the millimeter regime. For shorter wavelengths the surfaces of the antennae are typically too coarse, so that special telescopes are needed for wavelengths of 1 mm and below. The 30-m telescope on Pico Veleta (Fig. 1.22), with its exact surface shape, allows observations in the millimeter range. It is particularly used for molecular spectroscopy at these frequencies. Furthermore, important observations of high-redshift galaxies at 1.2 mm have been made with this telescope using the bolometer camera MAMBO. Similar observations are also conducted with the SCUBA (Submillimeter Common-User Bolometer Array) camera at the James Clerk Maxwell Telescope (JCMT; Fig. 1.23) on Mauna Kea, Hawaii. Due to its size and excellent location, the JCMT is arguably the most productive telescope in the submillimeter range; it is operated at wavelengths between 3 mm and 0.3 mm. With the SCUBA-camera, operating at 850 μm (0.85 mm), we can observe star-formation regions in distant galaxies for which the optical emission is nearly completely absorbed by dust in these sources. These dusty star-forming galaxies can be observed in the (sub-)millimeter regime of the electromagnetic spectrum even out to large redshifts, as will be discussed in Sect. 9.2.3.

To measure the tiny temperature fluctuations of the cosmic microwave background radiation one needs extremely stable observing conditions and low-noise detectors. In order to avoid the thermal radiation of the atmosphere as much as possible, balloons and satellites were constructed to operate instruments at very high altitude or in space. The American COBE (Cosmic Background Explorer) satellite measured the anisotropies of the CMB for the first time, at wavelengths of a few millimeters. In addition, the frequency spectrum of the CMB was precisely measured with instruments on COBE. The WMAP (Wilkinson Microwave Anisotropy Probe) satellite obtained, like COBE, a map of the full sky in the microwave regime, but at a significantly improved angular resolution and sensitivity. The first results from WMAP, published in February 2003, were an enormously important milestone for cosmology, as will be discussed in Sect. 8.6.5. Besides observing the CMB these missions are also of great importance for millimeter astronomy; these satellites not only measure the cosmic background radiation but of course also the microwave radiation of the Milky Way and of other galaxies.

1.3.2 Infrared Telescopes

In the wavelength range 1 μm $\lesssim \lambda \lesssim$ 300 μm, observations from the Earth's surface are always subject to very difficult conditions, if they are possible at all. The atmosphere has some windows in the near-infrared (NIR,

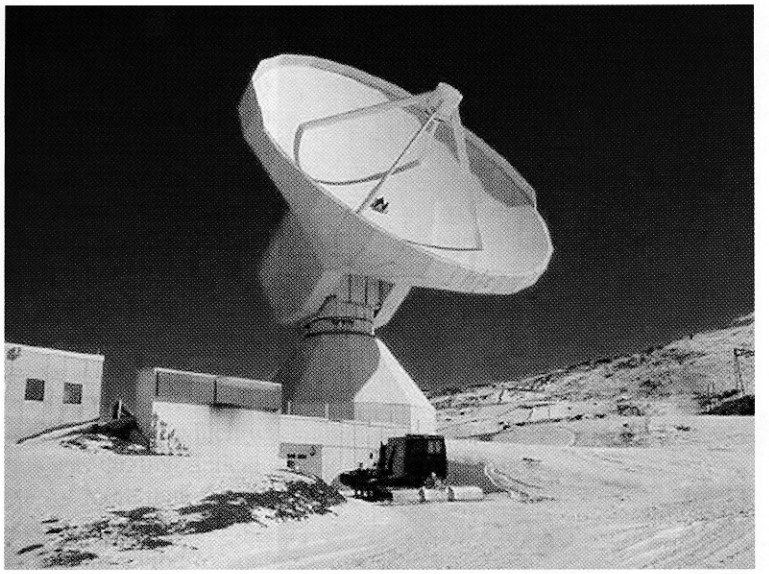

Fig. 1.22. The 30-m telescope on Pico Veleta was designed for observations in the millimeter range of the spectrum. This telescope, like all millimeter telescopes, is located on a mountain to minimize the column density of water in the atmosphere

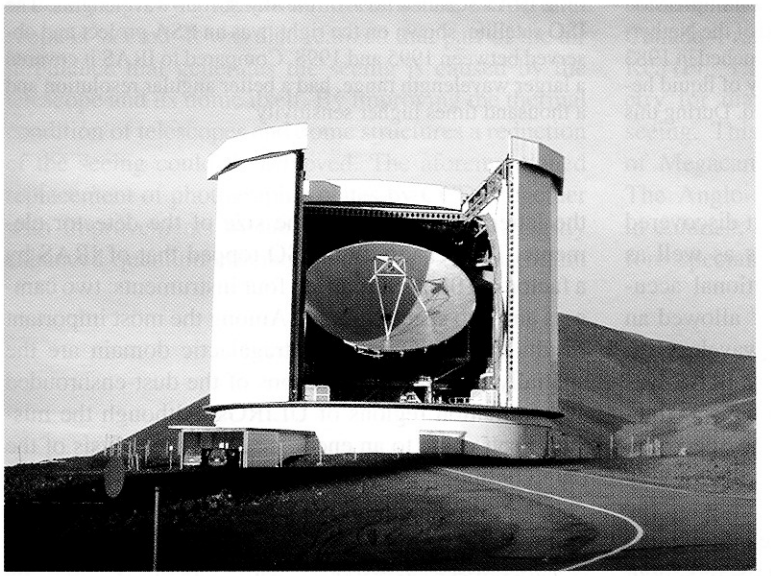

Fig. 1.23. The JCMT has a 15-m dish. It is protected by the largest single piece of Gore-Tex, which has a transmissivity of 97% at submillimeter wavelengths

$1\,\mu\text{m} \lesssim \lambda \lesssim 2.4\,\mu\text{m}$) which render ground-based observations possible. In the mid-infrared (MIR, $2.4\,\mu\text{m} \lesssim \lambda \lesssim 20\,\mu\text{m}$) and far-infrared (FIR, $20\,\mu\text{m} \lesssim \lambda \lesssim 300\,\mu\text{m}$) regimes, observations need to be carried out from outside the atmosphere, i.e., using balloons, high-flying airplanes, or satellites. The instruments have to be cooled to very low temperatures, otherwise their own thermal radiation would outshine any signal.

The first noteworthy observations in the far-infrared were made by the Kuiper Airborne Observatory (KAO), an airplane equipped with a 91-cm mirror which operated at altitudes up to 15 km. However, the breakthrough for IR astronomy had to wait until the launch of IRAS, the InfraRed Astronomical Satellite (Fig. 1.24). In 1983, with its 60-cm telescope, IRAS compiled the first IR map of the sky at 12, 25, 60, and 100 μm, at an angular

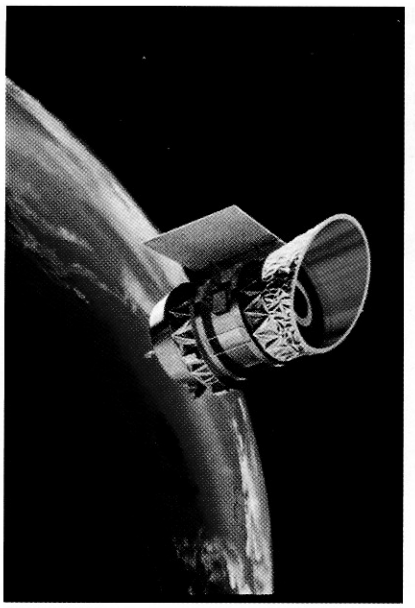

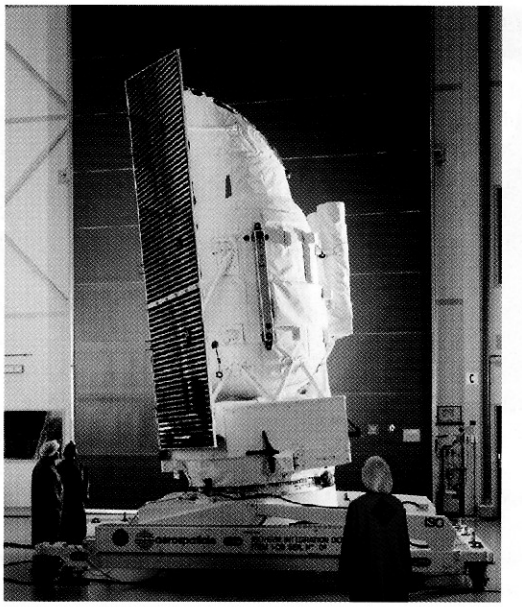

Fig. 1.24. The left-hand picture shows an artist's impression of IRAS in orbit. The project was a cooperation of the Netherlands, the USA, and Great Britain. IRAS was launched in 1983 and operated for 10 months; after that the supply of liquid helium, needed to cool the detectors, was exhausted. During this time IRAS scanned 96% of the sky at four wavelengths. The ISO satellite, shown on the right, was an ESA project and observed between 1995 and 1998. Compared to IRAS it covered a larger wavelength range, had a better angular resolution and a thousand times higher sensitivity

resolution of 30″ (2′) at 12 μm (100 μm). It discovered about a quarter of a million point sources as well as about 20 000 extended sources. The positional accuracy for point sources of better than ∼ 20″ allowed an identification of these sources at optical wavelengths. Arguably the most important discovery by IRAS was the identification of galaxies which emit the major fraction of their energy in the FIR part of the spectrum. These sources, often called IRAS galaxies, have a very high star-formation rate where the UV light of the young stars is absorbed by dust and then re-emitted as thermal radiation in the FIR. IRAS discovered about 75 000 of these so-called ultra-luminous IR galaxies (ULIRGs).

In contrast to the IRAS mission with its prime task of mapping the full sky, the Infrared Space Observatory ISO (Fig. 1.24) was dedicated to observations of selected objects and sky regions in a wavelength range 2.5–240 μm. Although the telescope had the same diameter as IRAS its angular resolution at 12 μm was about a hundred times better than that of IRAS, since the latter was limited by the size of the detector elements. The sensitivity of ISO topped that of IRAS by a factor ∼ 1000. ISO carried four instruments: two cameras and two spectrographs. Among the most important results from ISO in the extragalactic domain are the spatially-resolved observations of the dust-enshrouded star-formation regions of ULIRGs. Although the mission itself came to an end, the scientific analysis of the data continues on a large scale, since to date the ISO data are still unique in the infrared.

In 2003 a new infrared satellite was launched (the Spitzer Space Telescope) with capabilities that by far outperform those of ISO. With its 85-cm telescope, Spitzer observes at wavelengths between 3.6 and 160 μm. Its IRAC (Infrared Array Camera) camera, operating at wavelengths below ∼ 9 μm, has a field-of-view of $5.'2 \times 5.'2$ and 256×256 pixels, significantly more than the 32×32 pixels of ISOCAM on ISO that had a comparable wavelength coverage. The spectral resolution of the IRS (Infrared Spectrograph) instrument in the MIR is about $R = \lambda/\Delta\lambda \sim 100$.

1.3.3 Optical Telescopes

The atmosphere is largely transparent in the optical part of the electromagnetic spectrum ($0.3\ \mu\text{m} \lesssim \lambda \lesssim 1\ \mu\text{m}$), and thus we are able to conduct observations from the ground. Since for the atmospheric windows in the NIR one normally uses the same telescopes as for optical astronomy, we will thus not distinguish between these two ranges here.

Although optical astronomy has been pursued for many decades, it has evolved very rapidly in recent years. This is linked to a large number of technical achievements. A good illustration of this is the 10-m Keck telescope which was put into operation in 1993; this was the first optical telescope with a mirror diameter of more than 6 m. Constructing telescopes of this size became possible by the development of adaptive optics, a method to control the surface of the mirror. A mirror of this size no longer has a stable shape but is affected, e.g., by gravitational deformation as the telescope is steered. It was also realized that part of the air turbulence that generates the seeing is caused by the telescope and its dome itself. By improving the thermal condition of telescopes and dome structures a reduction of the seeing could be achieved. The aforementioned replacement of photographic plates by CCDs, together with improvements to the latter, resulted in a vastly enhanced quantum efficiency of $\sim 70\%$ (at maximum even more than 90%), barely leaving room for further improvements.

The throughput of optical telescopes has been immensely increased by designing wide-field CCD cameras, the largest of which nowadays have a field-of-view of a square degree and $\sim 16\,000 \times 16\,000$ pixels, with a pixel scale of $\sim 0\farcs2$. Furthermore, multi-object spectrographs have been built which allow us to observe the spectra of a large number of objects simultaneously. The largest of them are able to get spectra for several hundred sources in one exposure. Finally, with the Hubble Space Telescope the angular resolution of optical observations was increased by a factor of ~ 10. Further developments that will revolutionize the field even more, such as interferometry in the near IR/optical and adaptive optics, will soon be added to these achievements.

Currently, about 13 optical telescopes of the 4-m class exist worldwide. They differ mainly in their location and their instrumentation. For example, the Canada–France–Hawaii Telescope (CFHT) on Mauna Kea (Fig. 1.25) has been a leader in wide-field photometry for many years, due to its extraordinarily good seeing. This is again emphasized by the installation of Megacam, a camera with $18\,000 \times 18\,000$ pixels. The Anglo-Australian Telescope (AAT) in Australia, in contrast, has distinctly worse seeing and has therefore specialized, among other things, in multi-object

Fig. 1.25. Telescopes at the summit of Mauna Kea, Hawaii, at an altitude of 4200 m. The cylindrical dome to the left and below the center of the image contains the Subaru 8-m telescope; just behind it are the two 10-m Keck telescopes. The two large domes at the back house the Canada–France–Hawaii telescope (CFHT, 3.6 m) and the 8-m Gemini North. The telescope at the lower right is the 15-m James Clerk Maxwell submillimeter telescope (JCMT)

spectroscopy, for which the 2dF (two-degree field) instrument was constructed. Most of these telescopes are also equipped with NIR instruments. The New Technology Telescope (NTT, see Fig. 1.26) is especially noteworthy due to its SOFI camera, a near-IR instrument that has a large field-of-view of $\sim 5' \times 5'$ and an excellent image quality.

Hubble Space Telescope. To avoid the greatest problem in ground-based optical astronomy, the rocket scientist Hermann Oberth had already speculated in the 1920s about telescopes in space which would not be affected by the influence of the Earth's atmosphere. In 1946 the astronomer Lyman Spitzer took up this issue again and discussed the possibilities for the realization of such a project.

Shortly after NASA was founded in 1958, the construction of a large telescope in space was declared a long-term goal. After several feasibility studies and ESA's agreement to join the project, the HST was finally built. However, the launch was delayed by the explosion of the space shuttle *Challenger* in 1986, so that it did not take place until April 24, 1990. An unpleasant surprise came as soon as the first images were taken: it was found that the 2.4-m main mirror was ground into the wrong shape. This problem was remedied in December 1993 during the first "servicing mission" (a series of Space Shuttle missions to the HST; see Fig. 1.27), when a correction lens was installed. After this, the HST became one of the most successful and best-known scientific instruments.

The refurbished HST has two optical cameras, the WFPC2 (Wide-Field and Planetary Camera) and, since 2002, the ACS (Advanced Camera for Surveys). The latter has a field-of-view of $3.'4 \times 3.'4$, about twice as large as WFPC2, and 4000×4000 pixels. Another instrument was STIS (Space Telescope Imaging Spectrograph), operating mainly in the UV and at short optical wavelengths. Due to a defect it was shut down in 2004. The HST also carries a NIR instrument, NICMOS (Near Infrared Camera and Multi-Object Spectrograph). The greatly reduced thermal radiation, compared to that on the surface of the Earth, led to progress in NIR astronomy, albeit with a very small field-of-view.

HST has provided important insights into our Solar System and the formation of stars, but it has achieved milestones in extragalactic astronomy. With HST observations of the nucleus of M87 (Fig. 1.8), one has derived from the Doppler shift of the gas emission that the center of this galaxy contains a black hole of two billion solar masses. HST has also proven that black holes exist in other galaxies and AGNs. The enormously improved angular resolution has allowed us to study galaxies to a hitherto unknown level of detail. In this book we will frequently report on results that were achieved with HST.

Arguably the most important contribution of the HST to extragalactic astronomy are the Hubble Deep Fields.

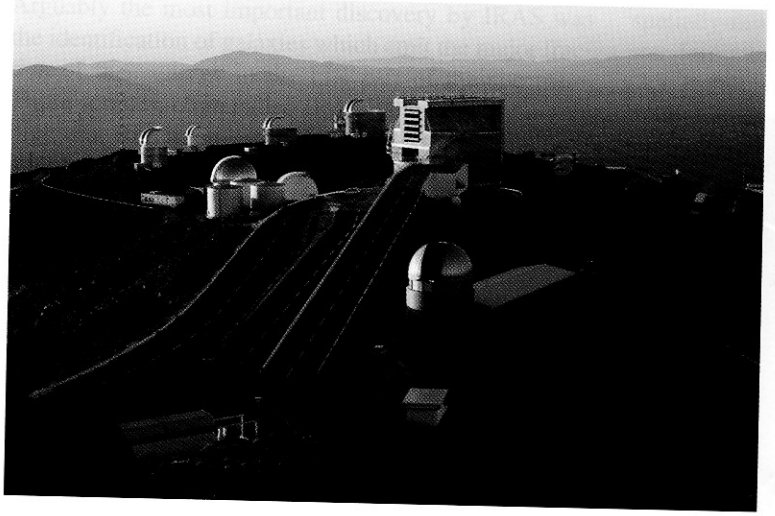

Fig. 1.26. The La Silla Observatory of ESO in Chile. On the peak in the middle, one can see the New Technology Telescope (NTT), a 3.5-m prototype of the VLT. The silvery shining dome to its left is the MPG/ESO 2.2-m telescope that is currently equipped with the Wide-Field Imager, a 8096^2 pixel camera with a 0.5° field-of-view. The picture was taken from the location of the 3.6-m telescope, the largest on La Silla

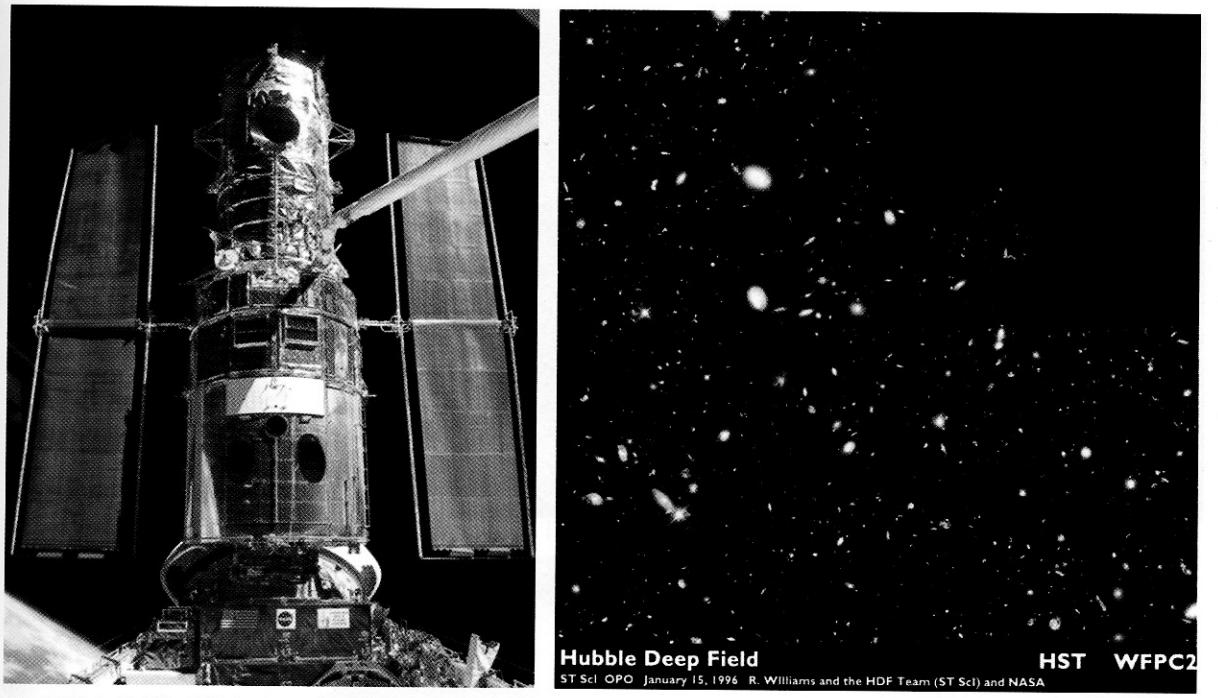

Fig. 1.27. Left: The HST mounted on the manipulator arm of the Space Shuttle during one of the repair missions. Right: The Hubble Deep Field (North) was taken in December 1995 and the data released one month later. To compile this multicolor image, which at that time was the deepest image of the sky, images from four different filters were combined

Scientists managed to convince Robert Williams, then director of the Space Telescope Science Institute, to use the HST to take a very deep image in an empty region of the sky, a field with (nearly) no foreground stars and without any known clusters of galaxies. At that time it was not clear whether anything interesting at all would come from these observations. Using the observing time that is allocated to the Director, the "director's discretionary time", in December 1995 HST was pointed at such a field in the Big Dipper, taking data for 10 days. The outcome was the Hubble Deep Field North (HDFN), one of the most important astronomical data sets, displayed in Fig. 1.27. From the HDFN and its southern counterpart, the HDFS, one obtains information about the early states of galaxies and their evolution. One of the first conclusions was that most of the early galaxies are classified as irregulars. In 2002, the Hubble Ultra-Deep Field (HUDF) was observed with the then newly installed ACS camera. Not only did it cover about twice the area of the HDFN but it was even deeper, by about one magnitude, owing to the higher sensitivity of ACS compared to WFPC2.

Large Telescopes. For more than 40 years the 5-m telescope on Mt. Palomar was the largest telescope in the western world – the Russian 6-m telescope suffered from major problems from the outset. The year 1993 saw the birth of a new class of telescope, of which the two Keck telescopes (see Fig. 1.28) were the first, each with a mirror diameter of 10 m.

The site of the two Kecks at the summit of Mauna Kea (at an altitude of 4200 m) provides ideal observing conditions for many nights per year. This summit is now home to several large telescopes. The new Japanese telescope Subaru, and Gemini North are also located here, as well as the aforementioned CFHT and JCMT. The significant increase in sensitivity obtained by Keck, especially in spectroscopy, permitted completely new insights, for instance through absorption line spectroscopy of quasars. Keck was also essential for the spectroscopic verification of innumer-

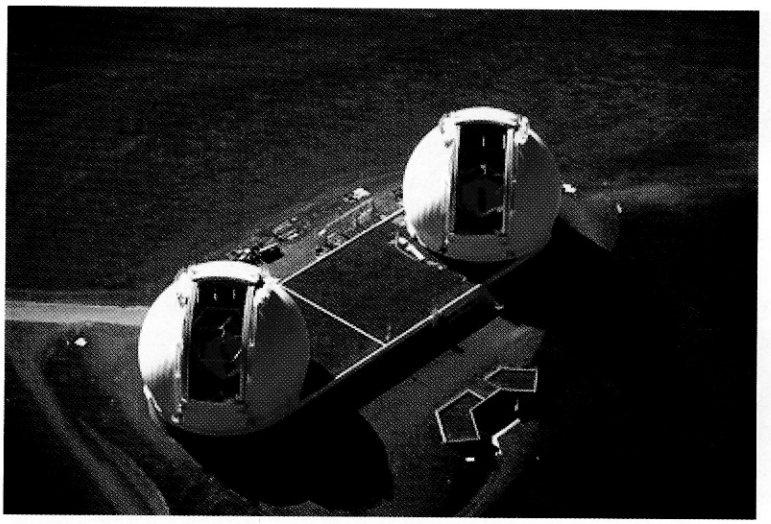

Fig. 1.28. The two Keck telescopes on Mauna Kea. With Keck I the era of large telescopes was heralded in 1993

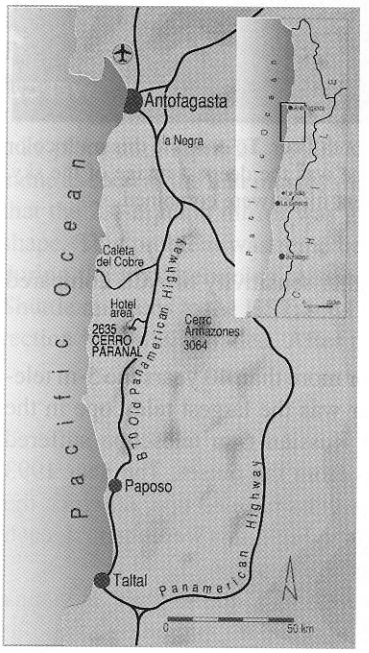

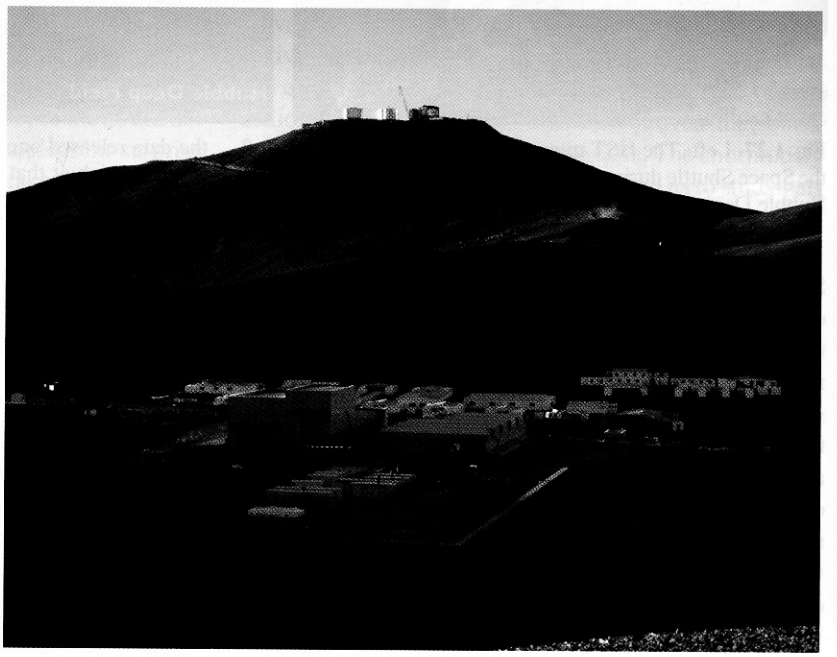

Fig. 1.29. The left panel shows a map of the location of the VLT on Cerro Paranal. It can be reached via Antofagasta, about a two-hour flight north of Santiago de Chile. Then another three-hour trip by car through a desert (see Fig. 1.30) brings one to the site. Paranal is shown on the right during the construction phase; in the foreground we can see the construction camp. The top of the mountain was flattened to get a leveled space (of diameter ~ 300 m) large enough to accommodate the telescopes and the facilities used for optical interferometry (VLTI)

able galaxies of redshift $z \gtrsim 3$, which are normally so dim that they cannot be examined with smaller telescopes.

The largest ground-based telescope project to date was the construction of the Very Large Telescope (VLT) of the European Southern Observatory (ESO), consist-

ing of four telescopes each with a diameter of 8.2 m. ESO already operates the La Silla Observatory in Chile (see Fig. 1.26), but a better location was found for the VLT, the Cerro Paranal (at an altitude of 2600 m). This mountain is located in the Atacama desert, one of the driest regions on Earth. To build the telescopes on the mountain a substantial part of the mountain top first had to be cut off (Fig. 1.29).

In contrast to the Keck telescopes, which have a primary mirror that is segmented into 36 hexagonal elements, the mirrors of the VLT are monolithic, i.e., they consist of a single piece. However, they are very thin compared to the 5-m mirror on Mt. Palomar, far too thin to be intrinsically stable against gravity and other effects such as thermal deformations. Therefore, as for the Kecks, the shape of the mirrors has to be controlled electronically (see Fig. 1.30, right). The monolithic structure of the VLT mirrors results in better image quality than that of the Keck telescopes, resulting in an appreciably simpler point-spread function.

Each of the four telescopes has three accessible foci; this way, 12 different instruments can be installed at the VLT at any time. Switching between the three instruments is done with a deflection mirror. The permanent installation of the instruments allows their stable operation.

The VLT (Fig. 1.31) also marks the beginning of a new form of ground-based observation with large optical telescopes. Whereas until recently an astronomer proposing an observation was assigned a certain number and dates of nights in which she could observe with the telescope, the VLT is mainly operated in the so-called service mode. The observations are performed by local astronomers according to detailed specifications that must be provided by the principal investigator of the observing program and the data are then transmitted to the astronomer at her home institution. A significant advantage of this procedure is that one can better account for special requirements for observing conditions. For example, observations that require very good seeing can be carried out during the appropriate atmospheric conditions. With service observing the chances of getting a useful data set are increased. At present about half of the observations with the VLT are performed in service mode. Another aspect of service observing is that the astronomer does not have to make the long journey (see Fig. 1.30), at the expense of also missing out on the adventure and experience of observing.

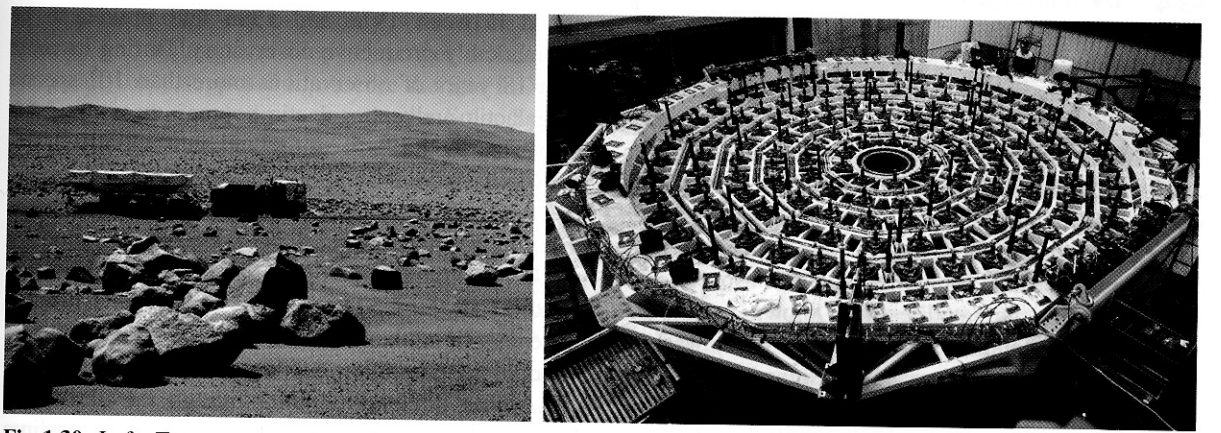

Fig. 1.30. Left: Transport of one of the VLT mirrors from Antofagasta to Paranal. The route passes through an extremely dry desert, and large parts of the road are not paved. The VLT thus clearly demonstrates that astronomers search for ever more remote locations to get the best possible observing conditions. Right: The active optics system at the VLT. Each mirror is supported at 150 points; at these points, the mirror is adjusted to correct for deformations. The primary mirror is always shaped such that the light is focused in an optimal way, with its form being corrected for the changing gravitational forces when the telescope changes the pointing direction. In adaptive optics, in contrast to active optics, the wavefront is controlled: the mirrors are deformed with high frequencies in such a way that the wavefront is as planar as possible after passing through the optical system. In this way one can correct for the permanently changing atmospheric conditions and achieve images at diffraction-limited resolution, though only across a fairly small region of the focal plane

Fig. 1.31. The Paranal Observatory after completion of the domes for the four VLT unit telescopes. The tracks seen in the foreground were installed for additional smaller telescopes that are now jointly used with the VLT unit telescopes for interferometric observations in the NIR

1.3.4 UV Telescopes

Radiation with a wavelength shorter than $\lambda \lesssim 0.3\,\mu\text{m} = 3000$ Å cannot penetrate the Earth's atmosphere but is instead absorbed by the ozone layer, whereas radiation at wavelengths below 912 Å is absorbed by neutral hydrogen in the interstellar medium. The range between these two wavelengths is the UV part of the spectrum, in which observation is only possible from space.

The Copernicus satellite (also known as the Orbiting Astronomical Observatory 3, OAO-3) was the first long-term orbital mission designed to observe high-resolution spectra at ultraviolet wavelengths. In addition, the satellite contained an X-ray detector. Launched on 21 August, 1972, it obtained UV spectra of 551 sources until its decommissioning in 1981. Among the achievements of the Copernicus mission are the first detection of interstellar molecular hydrogen H_2 and of CO, and measurements of the composition of the interstellar medium as well as of the distribution of OVI, i.e., five-time ionized oxygen.

The IUE (International Ultraviolet Explorer) operated between 1978 and 1996 and proved to be a remarkably productive observatory. During its more than 18 years of observations more than 10^5 spectra of galactic and extragalactic sources were obtained. In particular, the IUE contributed substantially to our knowledge of AGN.

The HST, with its much larger aperture, marks the next substantial step in UV astronomy, although no UV instrument is operational onboard HST after the failure of STIS in 2004. Many new insights were gained with the HST, especially through spectroscopy of quasars in the UV, insights into both the the quasars themselves and, through the absorption lines in their spectra, into the intergalactic medium along the line-of-sight towards the sources. In 1999 the FUSE (Far Ultraviolet Spectroscopic Explorer) satellite was launched. From UV spectroscopy of absorption lines in luminous quasars this satellite provided us with a plethora of information on the state and chemical composition of the intergalactic medium.

While the majority of observations with UV satellites were dedicated to high-resolution spectroscopy of stars and AGNs, the prime purpose of the GALEX satellite mission, launched in 2003, is to compile an extended photometric survey. GALEX observes at wavelengths $1350\,\text{Å} \lesssim \lambda \lesssim 2830\,\text{Å}$ and will perform a complete sky survey as well as observe selected regions of the sky with a longer exposure time. In addition, it will perform several spectroscopic surveys. The results from GALEX will be of great importance, especially for the study of the star-formation rate in nearby and distant galaxies.

1.3.5 X-Ray Telescopes

As mentioned before, interstellar gas absorbs radiation at wavelengths shortward of 912 Å, the so-called Lyman edge. This corresponds to the ionization energy of hydrogen in its ground state, which is 13.6 eV. Only at energies about ten times this value does the ISM become transparent again and this denotes the low-energy limit of the domain of X-ray astronomy. Typically, X-ray astronomers do not measure the frequency of light in Hertz (or the wavelength in μm), but instead photons are characterized by their energy, measured in electron volts (eV).

The birth of X-ray astronomy was in the 1960s. Rocket and balloon-mounted telescopes which were originally only supposed to observe the Sun in X-rays also received signals from outside the Solar System. UHURU, the first satellite to observe exclusively the cosmic X-ray radiation, compiled the first X-ray map of the sky, discovering about 340 sources. This catalog of point sources was expanded in several follow-up missions, especially by NASA's High-Energy Astrophysical Observatory (HEAO-1) which also detected a diffuse X-ray background radiation. On HEAO-2, also known as the Einstein satellite, the first Wolter telescope was used for imaging, increasing the sensitivity by a factor of nearly a thousand compared to earlier missions. The Einstein observatory also marked a revolution in X-ray astronomy because of its high angular resolution, about 2″ in the range of 0.1 to 4 keV. Among the great discoveries of the Einstein satellite is the X-ray emission of many clusters of galaxies that traces the presence of hot gas in the space between the cluster galaxies. The total mass of this gas significantly exceeds the mass of the stars in the cluster galaxies and therefore represents the main contribution to the baryonic content of clusters.

The next major step in X-ray astronomy was ROSAT (ROentgen SATellite; Fig. 1.32), launched in 1990. During the first six months of its nine-year mission ROSAT produced an all-sky map at far higher resolution than UHURU; this is called the ROSAT All Sky Survey. More than 10^5 individual sources were detected in this survey, the majority of them being AGNs. In the subsequent period of pointed observations ROSAT examined, among other types of sources, clusters of galaxies and AGNs. One of its instruments (PSPC) provided spectral information in the range between 0.1 and 2.4 keV at an angular resolution of $\sim 20''$, while the other (HRI) instrument had a much better angular resolution ($\sim 3''$) but did not provide any spectral information. The Japanese X-ray satellite ASCA (Advanced Satellite for Cosmology and Astrophysics), launched in 1993, was able to observe in a significantly higher energy range 0.5–12 keV and provided spectra of higher energy resolution, though at reduced angular resolution.

Since 1999 two new powerful satellites are in operation: NASA's Chandra observatory and ESA's XMM-Newton (X-ray Multi-Mirror Mission; see Fig. 1.32). Both have a large photon-collecting area and a high angular resolution, and they also set new standards in X-ray spectroscopy. Compared to ROSAT, the energy range accessible with these two satellites has been extended to 0.1–10 keV. The angular resolution of Chandra is about 0.″5 and thus, for the first time, comparable to that of optical telescopes. This high angular resolution already led to major discoveries in the early years of operation. For instance, well-defined sharp structures in the X-ray emission from gas in clusters of galaxies were discovered, and X-ray radiation from the jets of AGNs which had been previously observed in the radio was detected. Furthermore, Chandra discovered a class of X-ray sources, termed ultra-luminous compact X-ray sources (ULXs), in which we may be observing the formation of black holes (Sect. 9.6). XMM-Newton has a larger sensitivity compared to Chandra, however at a somewhat smaller angular resolution. Among the most important observations of XMM-Newton at the beginning of its operation was the spectroscopy of AGNs and of clusters of galaxies.

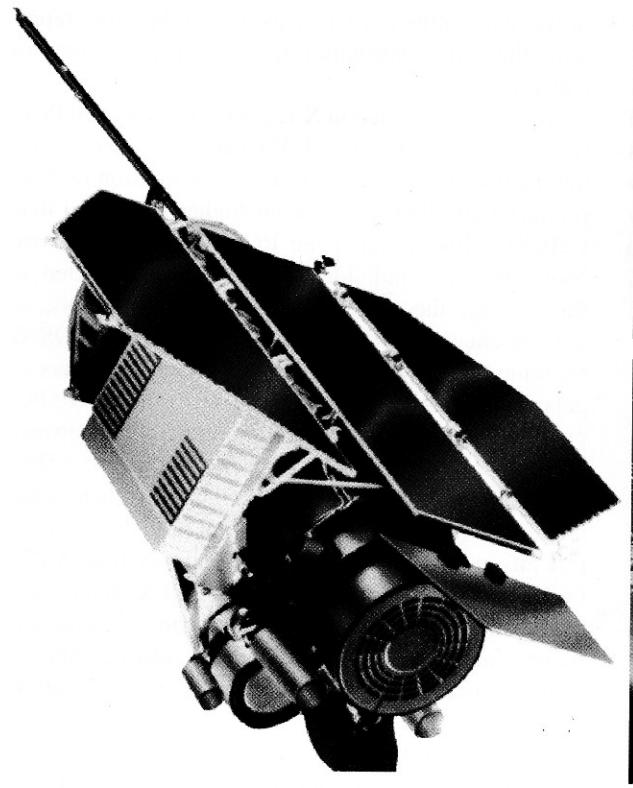

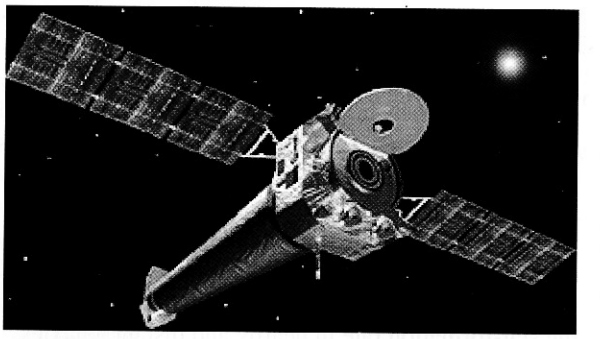

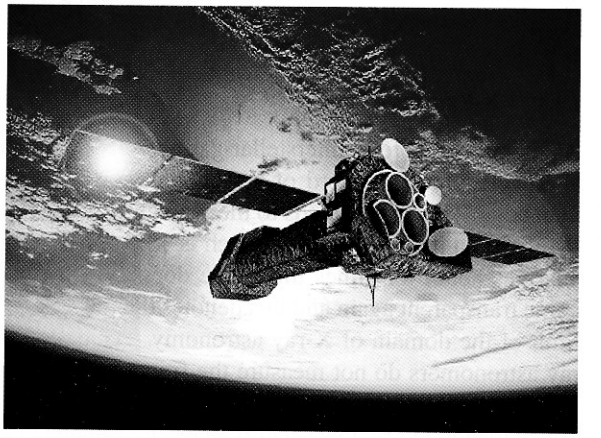

Fig. 1.32. Left: ROSAT, a German–US–British cooperation, was in orbit from 1990 to 1999 and observed in the energy range between 0.1 and 2.5 keV (soft X-ray). Upper right: Chandra was launched in July 1999. The energy range of its instruments lies between 0.1 and 10 keV. Its highly elliptical orbit permits long uninterrupted exposures. Lower right: XMM-Newton was launched in December 1999 and is planned to be used for 10 years. Observations are carried out with three telescopes at energies between 0.1 and 15 keV

1.3.6 Gamma-Ray Telescopes

The existence of gamma radiation was first postulated in the 1950s. This radiation is absorbed by the atmosphere, which is fortunate for the lifeforms on Earth. The first observations, carried out from balloons, rockets, and satellites, have yielded flux levels of less than 100 photons. Those gamma photons had energies in the GeV range and above.

Detailed observations became possible with the satellites SAS-2 and COS-B. They compiled a map of the galaxy, confirmed the existence of a gamma background radiation, and for the first time observed pulsars in the gamma range. The first Gamma Ray Bursts (GRB), extremely bright and short-duration flashes on the gamma-ray sky, were detected in the 1970s by military satellites. Only the Italian-Dutch satellite Beppo-SAX (1996 to 2002) managed to localize a GRB with sufficient accuracy to allow an identification of the source in other wavebands, and thus to reveal its physical nature; we will come back to this subject later, in Sect. 9.7.

An enormous advance in high-energy astronomy was made with the launch of the Compton Gamma Ray Observatory (CGRO; Fig. 1.33) in 1991; the observatory was operational for nine years. It carried four different instruments, among them the Burst And Transient Source Experiment (BATSE) and the Energetic Gamma Ray Experiment Telescope (EGRET). During its lifetime BATSE discovered more than 2000 GRBs and contributed substantially to the understanding of the nature of these mysterious gamma-ray flashes. EGRET

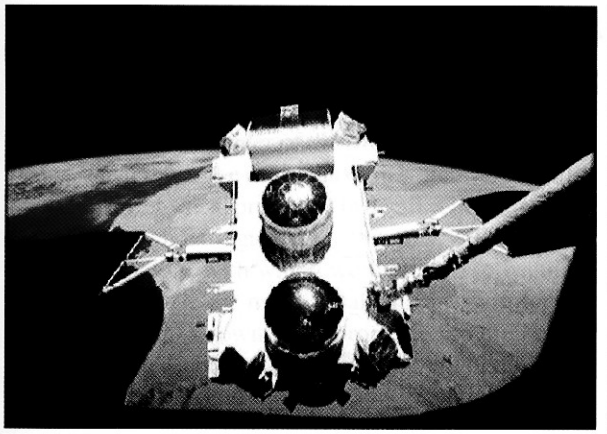

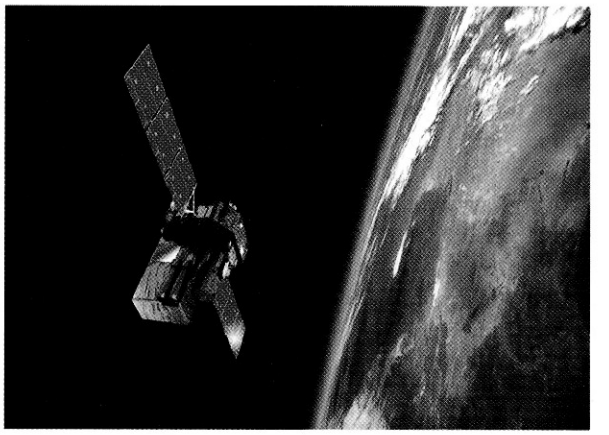

Fig. 1.33. The left image shows the Compton Gamma Ray Observatory (CGRO) mounted on the Space Shuttle manipulator arm. This NASA satellite carried out observations between 1991 and 2000. It was finally shut down after a gyroscope failed, and it burned up in the Earth's atmosphere in a controlled re-entry. ESA's Integral observatory, in operation since 2002, is shown on the right

discovered many AGNs at very high energies above 20 MeV, which hints at extreme processes taking place in these objects.

The successor of the CGRO, the Integral satellite, was put into orbit as an ESA mission by a Russian Proton rocket at the end of 2002. At a weight of two tons, it is the heaviest ESA satellite that has been launched thus far. It is primarily observing at energies of 15 keV to 10 MeV in the gamma range, but has additional instruments for observation in the optical and X-ray regimes.